

63-3-3

403486

ARL-63-26

403 486

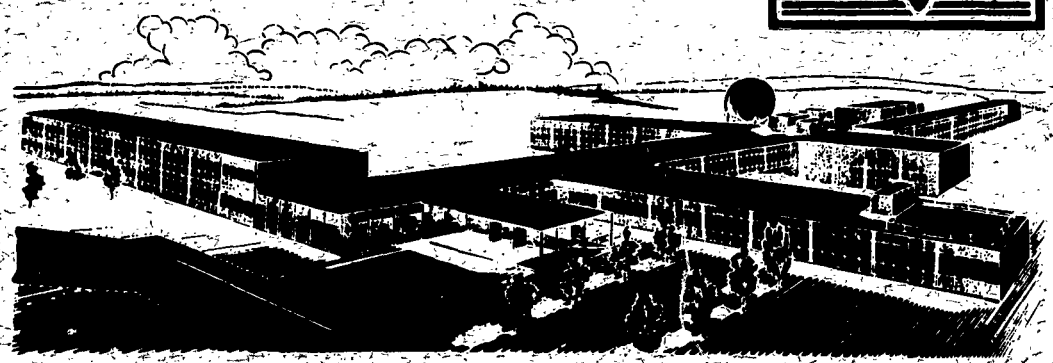
# AN INVESTIGATION OF A THREE-DIMENSIONAL TURBULENT BOUNDARY LAYER IN HYPERSONIC FLOW

GENNARO F. AEILLO  
POLYTECHNIC INSTITUTE OF BROOKLYN  
FREEPORT, NEW YORK

FEBRUARY 1963

ASTIA  
MAY 7 1963  
TISIA A

AERONAUTICAL RESEARCH LABORATORIES  
OFFICE OF AEROSPACE RESEARCH  
UNITED STATES AIR FORCE



CATALOGED BY ASTIA  
AS AD NO.

**ARL 63-26**

**AN INVESTIGATION OF A THREE-DIMENSIONAL TURBULENT  
BOUNDARY LAYER IN HYPERSONIC FLOW**

**GENNARO F. AIELLO  
POLYTECHNIC INSTITUTE OF BROOKLYN  
FREEPORT, NEW YORK**

**FEBRUARY 1963**

**CONTRACT AF 33(616)-7661  
PROJECT 7064  
TASK 7064-01**

**AERONAUTICAL RESEARCH LABORATORIES  
OFFICE OF AEROSPACE RESEARCH  
UNITED STATES AIR FORCE  
WRIGHT-PATTERSON AIR FORCE BASE, OHIO**

## FOREWORD

This interim report was prepared by Mr. Gennaro Aiello, Research Assistant, and presents research carried out under Contract No. AF 33(616)-7661, "Research on Thermal and Aerodynamic Effects at Hypersonic Mach Numbers in High Speed Flow," Project No. 7064, "Aerothermodynamic Investigations," Task No. 7064-01, "Research on Hypersonic Flow Phenomena." This contract is administered by the Aeronautical Research Laboratories, Office of Aerospace Research, United States Air Force, and is partially supported by the Ballistic Systems Division. Colonel Andrew Boreske, Jr. of the Hypersonic Research Laboratory, ARL, is the contract monitor.

The author wishes to express appreciation to Professor Paul A. Libby for his guidance and suggestions, and to Research Assistant Professor Robert J. Cresci for his invaluable assistance in carrying out the investigation. The author would also like to thank Mr. Samuel Lederman and the instrumentation group for their contributions to the test program and to the data reduction.

## ABSTRACT

Turbulent heating rates have been measured by means of the shrouded model technique on a blunted cone at angle of attack. The Reynolds number, based on conditions at the stagnation point, was varied from  $1.7 \cdot 10^6$  to approximately  $3.7 \cdot 10^6$ . The enthalpy ratio (stagnation to wall) varied from 2.1 to approximately 1.5.

The experimental data are compared to the flat-plate reference-enthalpy theory applied along the inviscid streamlines. It is shown that this relatively simple method is in reasonable agreement with the data.

## TABLE OF CONTENTS

SECTION		PAGE
I	INTRODUCTION . . . . .	1
II	MODEL DESIGN AND TEST PROCEDURES . . . . .	3
III	THEORETICAL ANALYSIS . . . . .	16
IV	COMPARISON BETWEEN THEORY AND EXPERIMENT . . . . .	24
V	CONCLUSIONS . . . . .	41
VI	REFERENCES . . . . .	41

## LIST OF ILLUSTRATIONS

FIGURE		PAGE
1	Test arrangement . . . . .	5
2	Model design	
	(a) Pressure model . . . . .	6
	(b) Heat transfer . . . . .	7
3	Coordinate system . . . . .	8
4	Circumferential pressure distribution	
	(a) $\bar{s} = 1.0$ . . . . .	9
	(b) $\bar{s} = 1.2$ . . . . .	10
	(c) $\bar{s} = 1.4$ . . . . .	11
	(d) $\bar{s} = 1.6$ . . . . .	12
	(e) $\bar{s} = 1.8$ . . . . .	13
	(f) $\bar{s} = 2.0$ . . . . .	14
5	Perturbation coefficients . . . . .	20
6	Nu vs. $\tilde{N}_r$ , $\theta = 20^\circ$	
	(a) Thermocouple 21, ( $\bar{s} = 1.45$ ) . . . . .	25
	(b) Thermocouple 25, ( $\bar{s} = 1.65$ ) . . . . .	25
	(c) Thermocouple 27, ( $s = 1.75$ ) . . . . .	26
7	Nu vs. $\tilde{N}_r$ , $\theta = 80^\circ$	
	(a) Thermocouple 17, ( $\bar{s} = 1.25$ ) . . . . .	27
	(b) Thermocouple 25, ( $\bar{s} = 1.65$ ) . . . . .	28
	(c) Thermocouple 27, ( $s = 1.75$ ) . . . . .	29
8	Nu vs. $\tilde{N}_r$ , $\theta = 100^\circ$	
	(a) Thermocouple 22, ( $\bar{s} = 1.55$ ) . . . . .	30
	(b) Thermocouple 30, ( $\bar{s} = 1.95$ ) . . . . .	30
	(c) Thermocouple 32, ( $\bar{s} = 2.05$ ) . . . . .	31

**LIST OF ILLUSTRATIONS (Contd)**

<b>FIGURE</b>		<b>PAGE</b>
9	Nu vs. $\tilde{N}_r$ , $\theta = 160^\circ$	
	(a) Thermocouple 20, ( $\bar{s} = 1.45$ ) . . . . .	31
	(b) Thermocouple 22, ( $\bar{s} = 1.55$ ) . . . . .	32
	(c) Thermocouple 26, ( $\bar{s} = 1.75$ ) . . . . .	32
10	$Nu/\tilde{N}_r^{4/5}$ vs. $\bar{s}$	
	(a) $\theta = 20^\circ$ . . . . .	33
	(b) $\theta = 80^\circ$ . . . . .	34
	(c) $\theta = 100^\circ$ . . . . .	35
	(d) $\theta = 160^\circ$ . . . . .	36

LIST OF TABLES

<u>TABLE</u>		<u>PAGE</u>
1	Location of Pressure Taps and Thermocouples . . . . .	21
2.0	Streamline Coordinates . . . . .	22

## LIST OF SYMBOLS

$C_p$	coefficient of specific heat at constant pressure
$h$	enthalpy
$\bar{h}$	$h/h_{s_e}$
$k$	coefficient of thermal conductivity
$K$	$1 - (1 - \sigma^{\frac{1}{2}})[(1 - \bar{h})/(1 - \bar{h}_w)]$
$m$	coordinate normal to the wall
$Nu$	$q_w C_{p_{s_e}} R_o / k_{f_e} (h_{s_e} - h_w)$ , Nusselt number
$N_r$	$\rho_{s_e} \sqrt{h_{s_e}} R_o / \mu_{s_e}$ , Reynolds number
$\tilde{N}_r$	$N_r \phi_{s_e}$
$p$	pressure
$\bar{p}$	$p_e/p_s$
$q_w$	heat transfer per unit area per unit time
$R_o$	reference length (radius of spherical nose)
$s$	distance along the surface
$\bar{s}$	$s/R_o$
$v$	velocity
$v_m$	$2\gamma p_s / (\gamma - 1) \rho_s$
$v_r$	$v_r/v_m$
$v_s$	axial velocity component
$v_o, v_1, w_1$	perturbation coefficients
$\bar{v}$	$v/v_m$
$w$	circumferential velocity component
$\bar{w}$	$w/v_m$

## LIST OF SYMBOLS (Contd)

$\alpha$	angle of attack
$\beta$	circumferential coordinate, wind axes
$\gamma$	ratio of specific heats
$\epsilon$	$\tan^{-1} w/v_r$ , streamline direction
$\theta$	circumferential coordinate, body axes
$\mu$	coefficient of viscosity
$\mu_e$	$\mu_e/\mu_{s_e}$
$\rho$	mass density
$\rho_e$	$\rho_e/\rho_{s_e}$
$\sigma$	Prandtl number
$\varphi$	axial coordinate, body axes
$\varphi_{s_e}$	$p_s/\rho_{s_e} h_{s_e}$
$\psi$	axial coordinate, wind axes

### Subscripts

e	conditions external to the boundary layer
s	stagnation conditions
w	wall conditions

### Superscripts

( )'	denotes conditions evaluated at the state corresponding to the reference enthalpy
------	---

## SECTION I

### INTRODUCTION

The practical importance of blunt bodies for the hypersonic flow regime has resulted in extensive work aimed at determining methods with which the high heat transfer rates such a vehicle encounters can be predicted. The boundary layer in this instance will be characterized by high stagnation-to-wall enthalpy ratios, low Mach numbers external to the boundary layer, and strong, favorable pressure gradients. In general, the flow will be three-dimensional; further laminar, transitional, and fully developed turbulent boundary layers are all of importance.

It is well-known that the analytical means of dealing with this broad problem have been developed in a succession of investigations into each of the particular features involved. The laminar compressible boundary layer under the subject conditions can be handled satisfactorily for two-dimensional and axisymmetric flows, due to the work of Lees<sup>(1)</sup>, Probstein<sup>(2)</sup>, and Fay and Riddell<sup>(3)</sup>. A method of attack for the general three-dimensional case, however, did not appear until relatively recently<sup>(4)</sup>.

Several approaches as to the description of the three-dimensional boundary layer were suggested initially. Hayes<sup>(5)</sup>, Moore<sup>(6)</sup>, and Howarth<sup>(7)</sup>, with varying opinions as to the most desirable coordinate system to be used, provided the basis for much of the subsequent effort. The early attempts, such as those reviewed in reference 8, dealt primarily with flows that exhibited some symmetry, or that could be approximated by perturbations of two-dimensional flows. Subsequently, some quantitative results were obtained for special cases, namely, the flow near the stagnation line of a yawed infinite cylinder<sup>(9)</sup>, near the windward streamline in the symmetry plane of a yawed cone<sup>(10)</sup>, and the flow at a general three-dimensional stagnation point in the presence of a cold wall<sup>(11)</sup>. The case of a blunt body was investigated, for small angles of attack, in reference 12.

---

Manuscript released 17 December 1962 by the authors for publication as an ARL Technical Documentary Report.

It was pointed out in reference 5 and restated in reference 4, that a three-dimensional boundary layer can be treated as a perturbation of two-dimensional or axisymmetric flows if: a) the three-dimensional effects in the inviscid flow can be linearized; b) the curvature of the outer edge streamline has a small component in the plane tangent to the surface of the body. Then, provided a cylindrical coordinate system with origin at the stagnation point is used, the problem can be handled.

Vaglio-Laurin shows in reference 4, however, that in the presence of a cold wall and moderate Mach numbers external to the boundary layer, a general three-dimensional streamline pattern can be dealt with. For these conditions it is demonstrated that with the inviscid streamlines and normals thereto as the coordinate system, the approximation of zero crossflow in the boundary layer is valid. The problem then becomes one of establishing the location of these streamlines, of evaluating the metric of the coordinate system, and of applying two-dimensional solutions along the streamlines. This approach will be used in this paper. The method used to determine the streamlines, however, is not that of reference 4 but one which is suggested in reference 13 and which has the advantage of ease of application, though perhaps it is not quite as accurate. The method will be discussed in greater detail in a later section.

As was mentioned previously the boundary layer on a blunt body under the conditions considered would, in practice, become turbulent. Unlike the situation of the laminar boundary layer most of the analyses available for turbulent boundary layers, such as those reviewed in reference 14, for example, are limited to two-dimensional incompressible flows. Within the past few years satisfactory correlations between compressible and incompressible turbulent boundary layers have been developed by Englert<sup>(15)</sup> and Mager<sup>(16)</sup>. Attempts by Mager<sup>(17)</sup> and Braun<sup>(18)</sup> to extend the analysis to three-dimensional (incompressible and compressible) flows, respectively, by applying two-dimensional integral techniques along streamlines, have not provided conclusive quantitative results because of uncertainty in the selection of velocity profiles for the crossflow. Vaglio-Laurin, in reference 19 shows that for highly cooled surfaces and moderate

Mach numbers external to the boundary layer, the zero crossflow approximation is also valid for arbitrary streamline patterns in turbulent flows. In fact, as stated therein, significantly smaller crossflows are to be expected in a turbulent boundary layer than in a laminar layer in the presence of favorable pressure gradients.

The purpose of the present work is to measure the pressure and heat transfer distributions on a spherically capped cone at angle of attack with the shrouded model technique of reference 20. The aim was not to simulate a particular pressure distribution, but merely to provide a three-dimensional flow to which theoretical analysis can be applied and compared. The same experimental technique was used in reference 21 for laminar, transitional and turbulent flows on a similar spherically capped cone at zero angle of attack. It was concluded therein that the flat-plate reference-enthalpy method provided more accurate results than a more complicated method based on reference 19. This result, which has been qualitatively confirmed by several authors (reference 22 for example) suggested the use of the simpler method here also.

## SECTION II

### MODEL DESIGN AND TEST PROCEDURES

The results presented here were obtained with the shrouded model technique in conjunction with the hypersonic facility of the Polytechnic Institute of Brooklyn. The overall facility and the pebble-bed heater employed are described in references 23 and 24 respectively. A schematic of the test arrangement is shown in Figure 1.

The models tested and the instrumentation layout are shown in Figures 2a and 2b. Since the flow considered is three-dimensional, a relatively large number of data points were required on the body. This made it impractical to attempt to instrument a single model with both the pressure taps and thermocouples required. Therefore, two identical

models were made of 304 stainless steel; one with pressure taps (Figure 2a) and the second with thermocouples (Figure 2b). In addition, the thermocouple model was instrumented with two pressure taps to provide a means of checking the location of the model with respect to the shroud. The coordinate system used for the model is shown in Figure 3.

The heat transfer measurements were obtained by means of a transient, one-dimensional heat conduction technique described in reference 25. The method consisted of recording the surface temperature of a one-dimensional plug, partially insulated from the surrounding model, as a function of time. The heat transfer rates were then computed as a function of time by an EASE analog computer. The surface temperature history was fed into the computer as one of the boundary conditions; the inside surface was assumed to be insulated. The thermal properties of the metal were considered constant.

The pressures were measured with a transducer and recorded on a Honeywell Visicorder. Because of the large number of taps several tests were required to cover all the data points. The pressure distribution, non-dimensionalized with respect to the stagnation pressure, was found to be independent of stagnation pressure over the entire range of stagnation pressure considered.

Though no attempt was made to simulate a particular three-dimensional flow, the shroud was designed to obtain a Newtonian pressure distribution with the model at zero angle of attack. The three-dimensional flow was obtained by putting the model at a geometric angle of attack of  $1.5^\circ$ . The peripheral pressure distribution at six stations on the body are shown in Figures 4a through 4f.

In order to obtain the variation of heat transfer with Reynolds number, the Reynolds number was varied continuously during the run by changing the stagnation pressure. The data are presented in terms of a Nusselt number defined by

$$Nu = q_w C_{p_s} R_o / K_{s_e} (h_{s_e} - h_w)$$

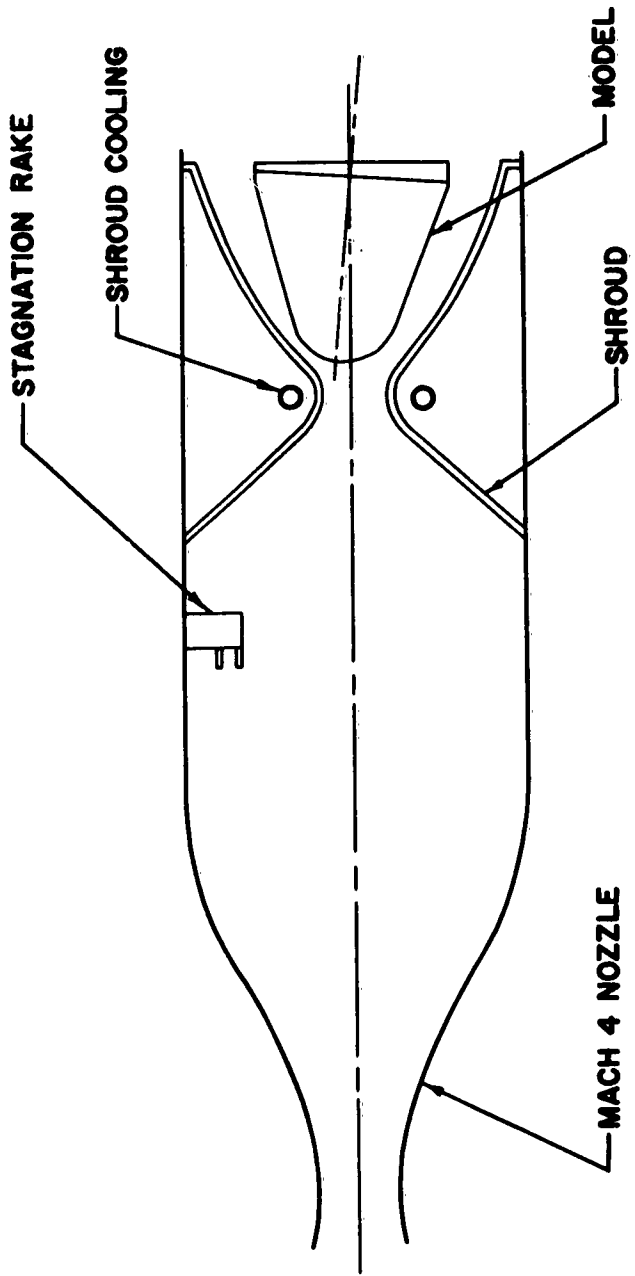
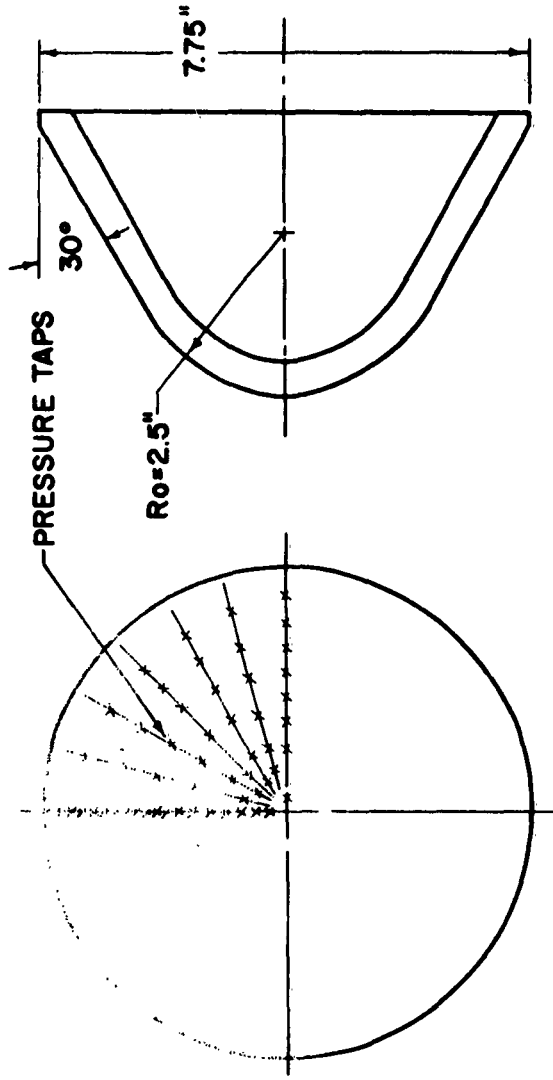


Fig. 1. Test Arrangement



**NOTE: ALL FOUR QUADRANTS HAVE  
 THE SAME INSTRUMENTATION**

Fig. 2a. Model Design - Pressure Model

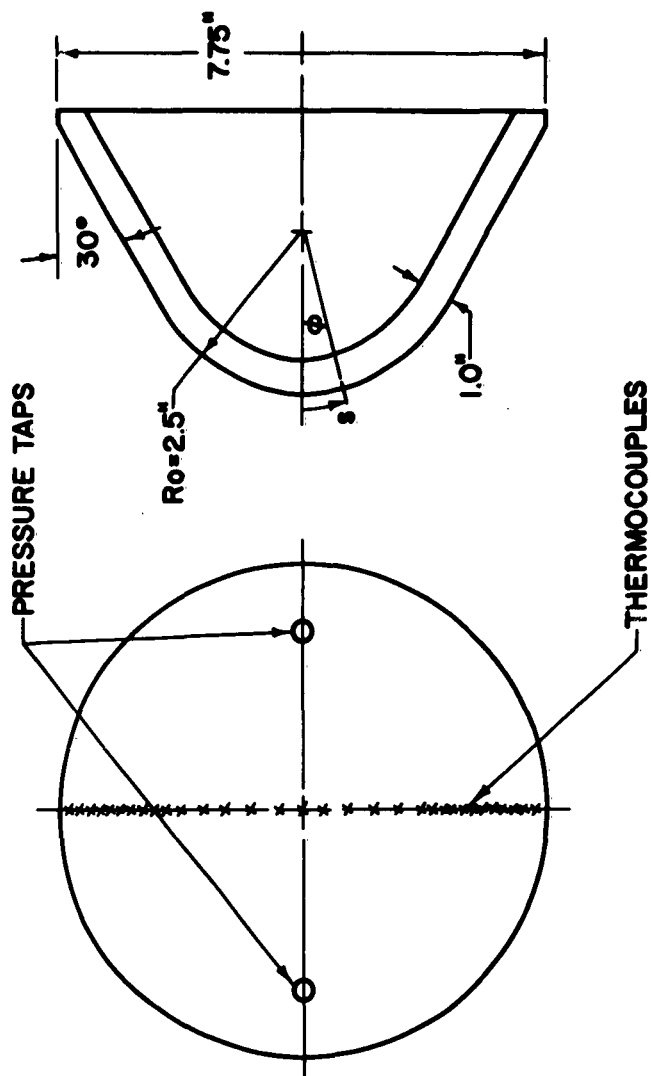


Fig. 2b. Model Design - Heat Transfer

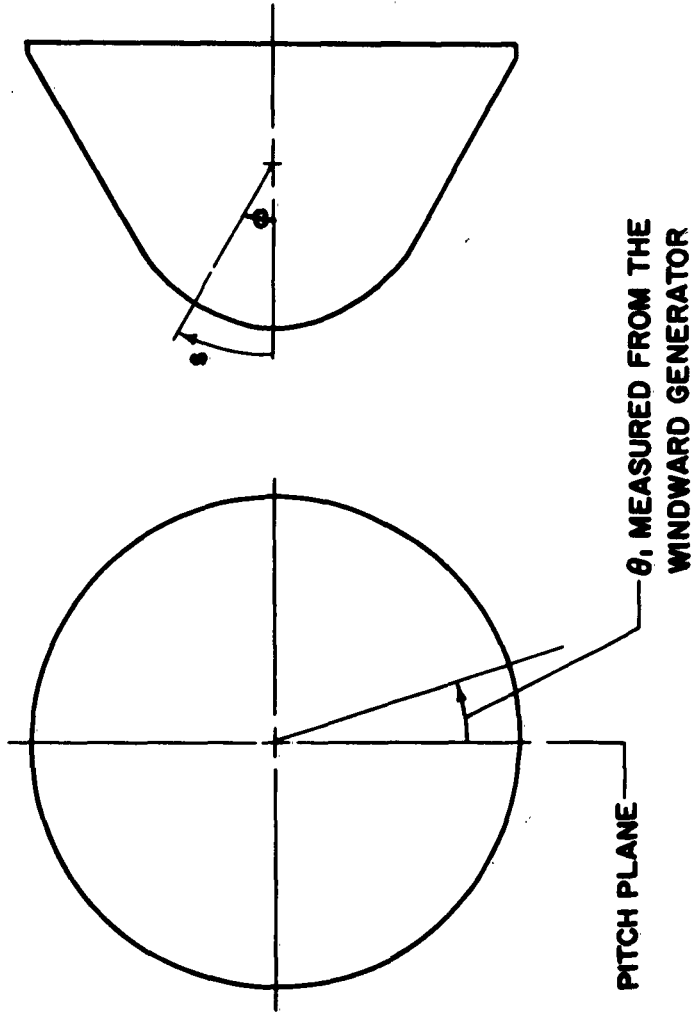


Fig. 3. Coordinate System

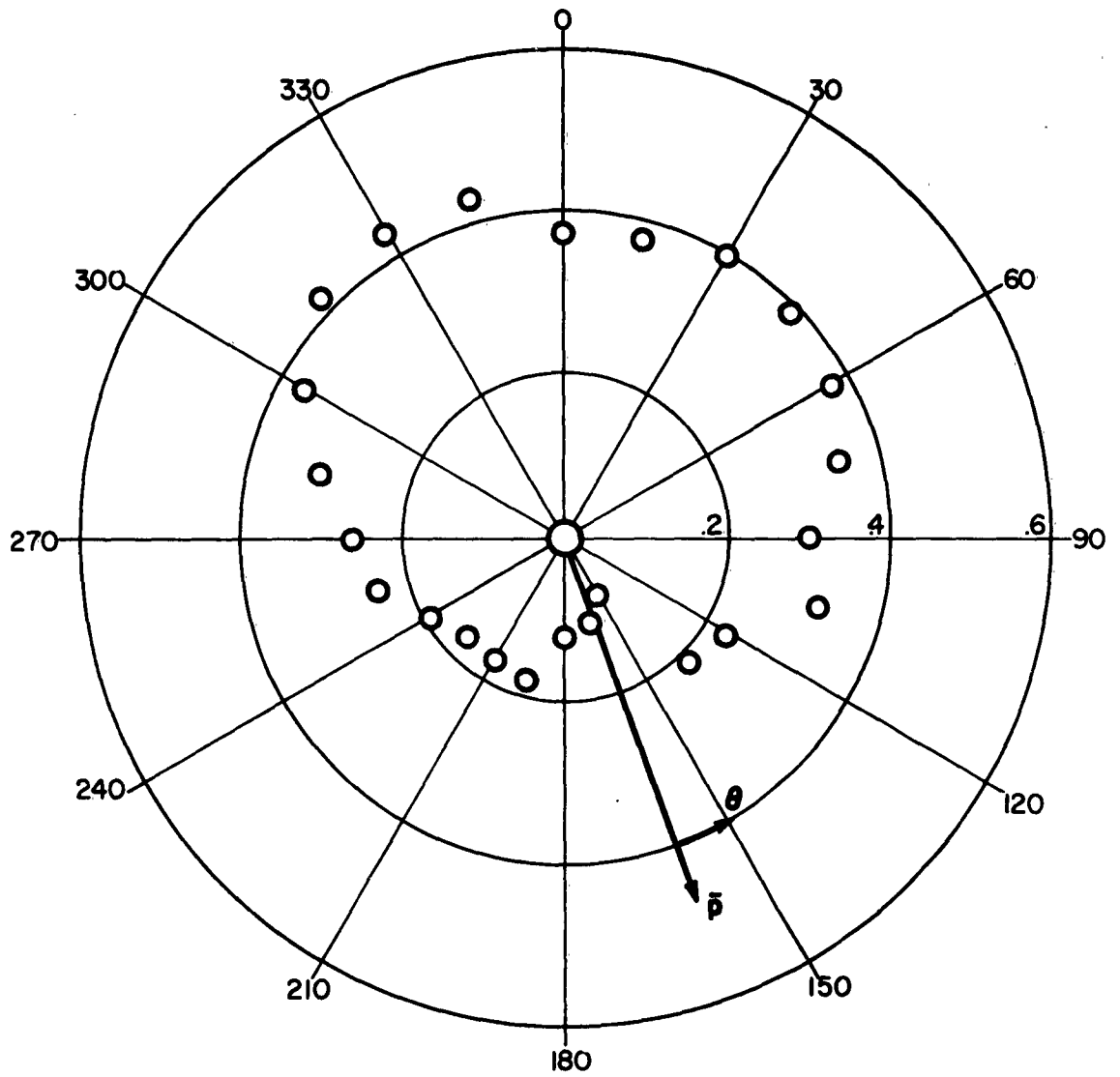


Fig. 4a. Circumferential Pressure Distribution -  $\bar{s} = 1.0$

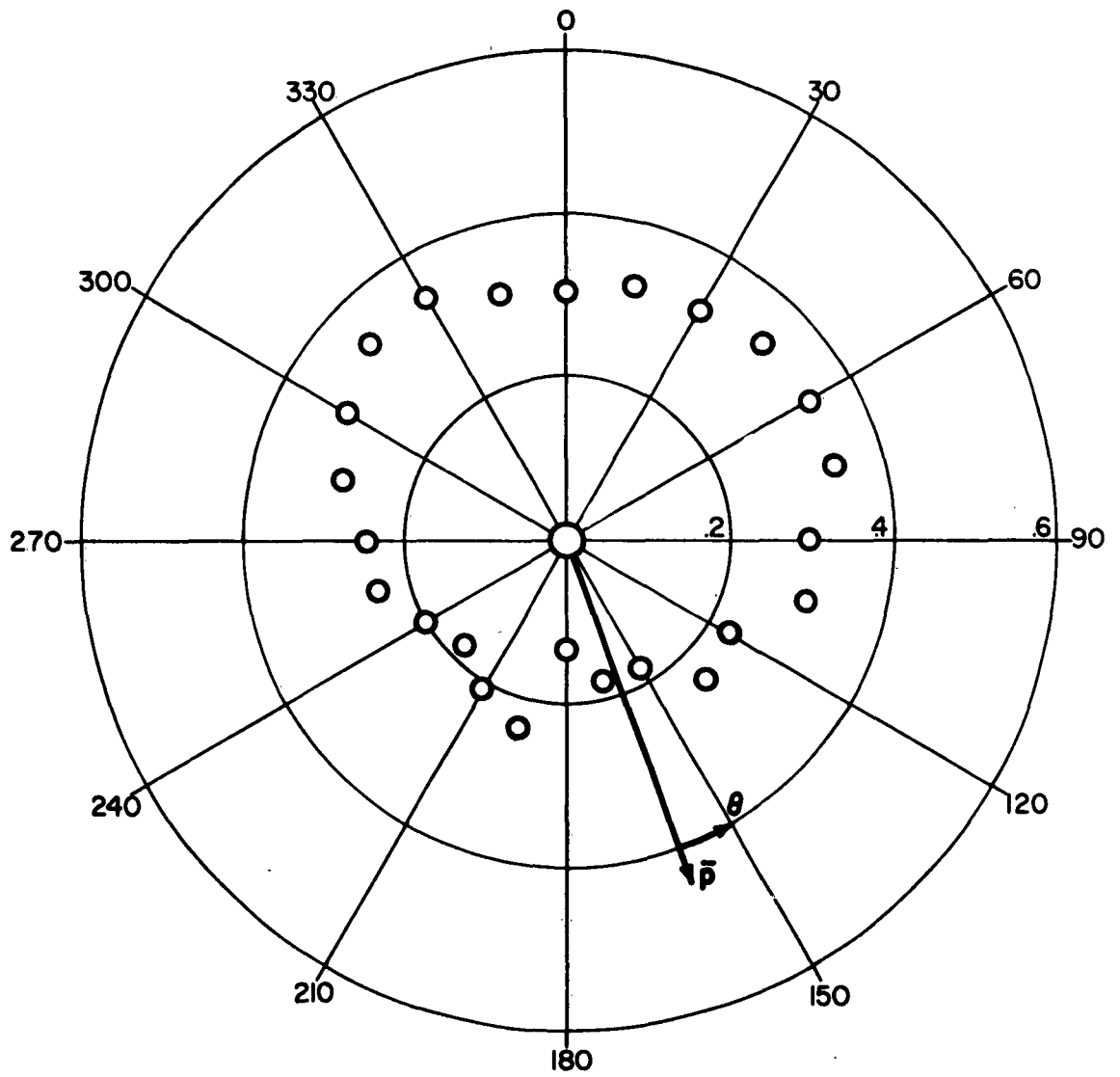


Fig. 4b. Circumferential Pressure Distribution -  $\bar{s} = 1.2$

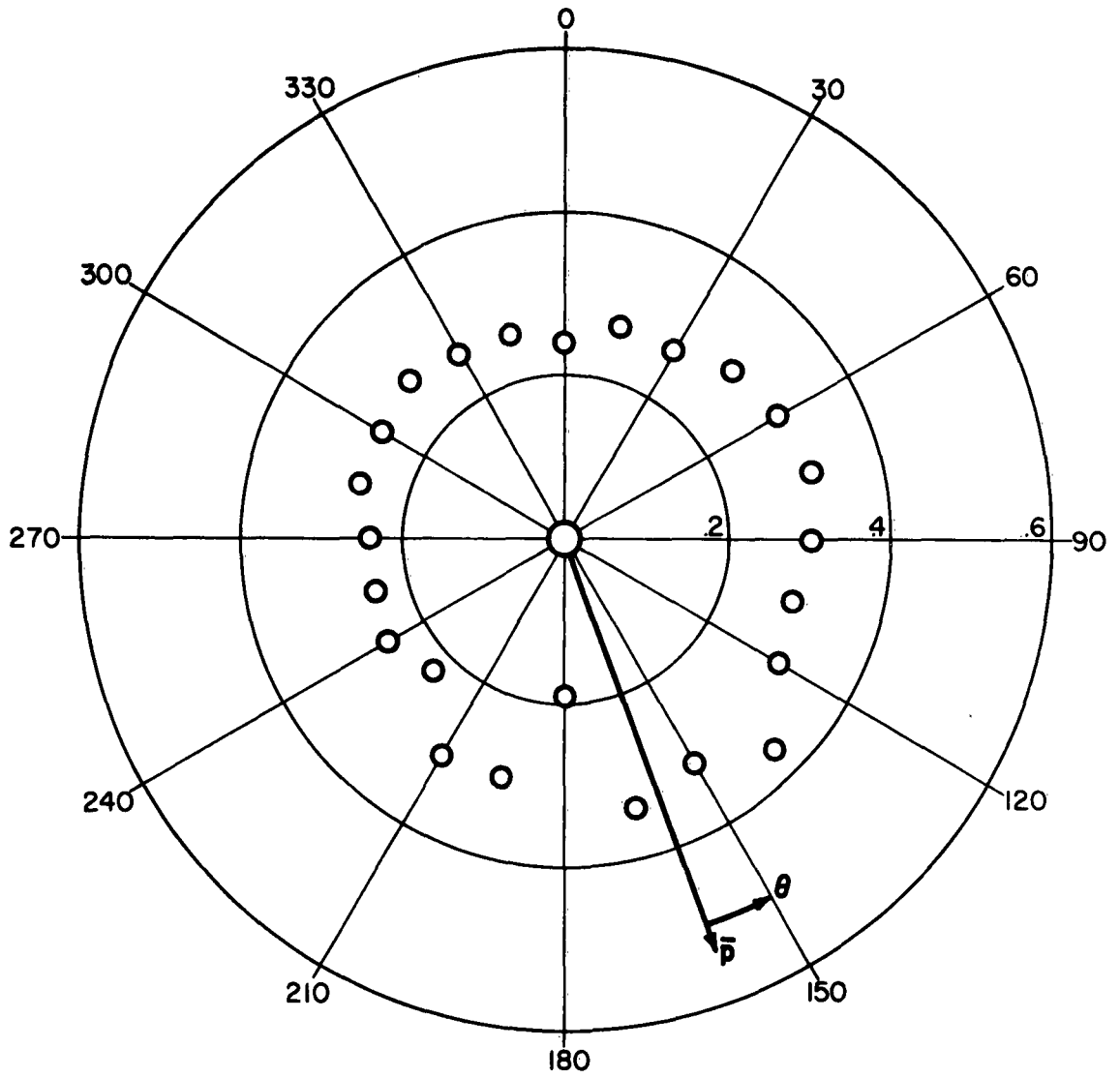


Fig. 4c. Circumferential Pressure Distribution -  $\bar{s} = 1.4$

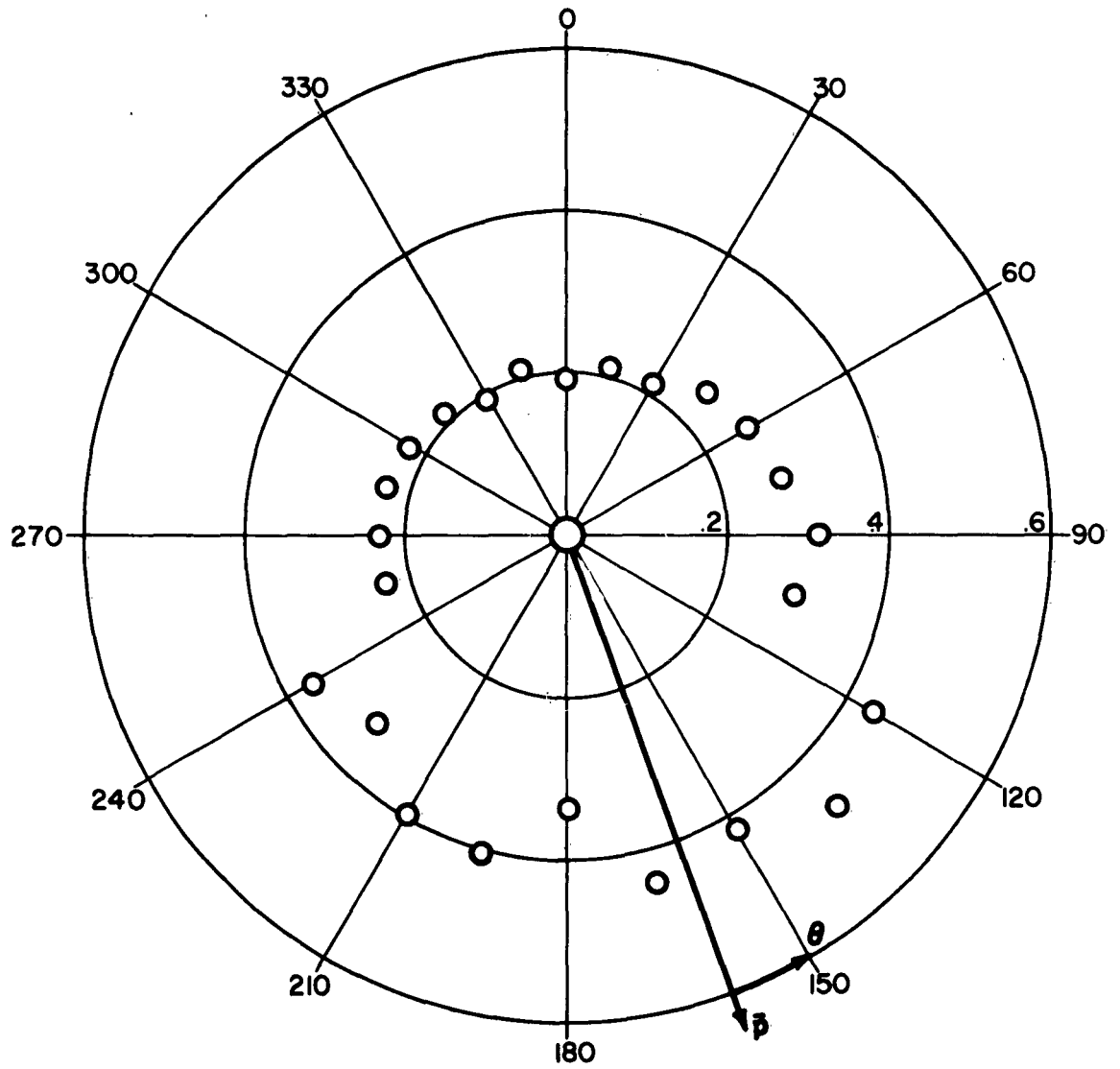


Fig. 4d. Circumferential Pressure Distribution -  $\bar{s} = 1.6$

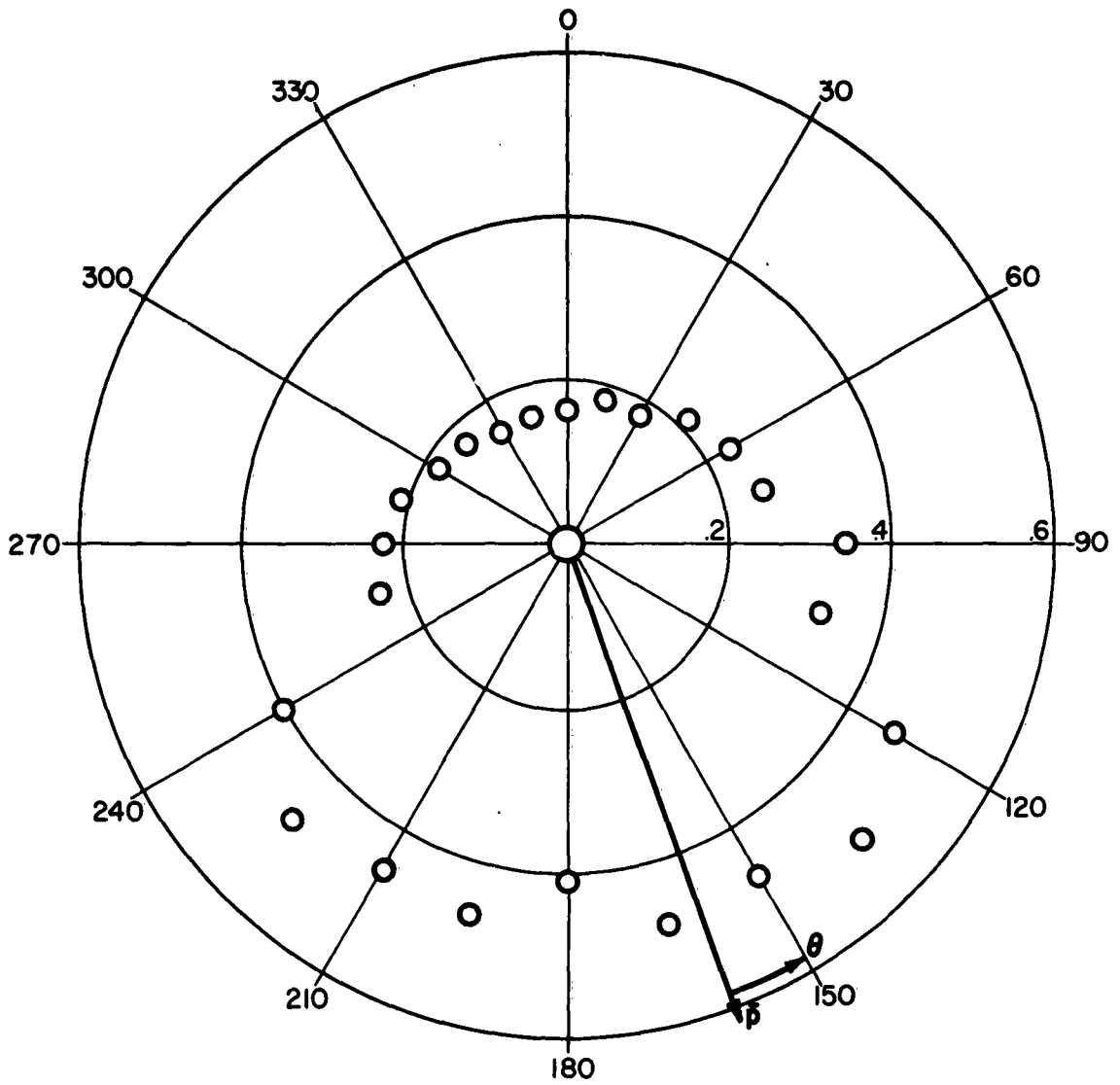


Fig. 4e. Circumferential Pressure Distribution -  $\bar{s} = 1.8$

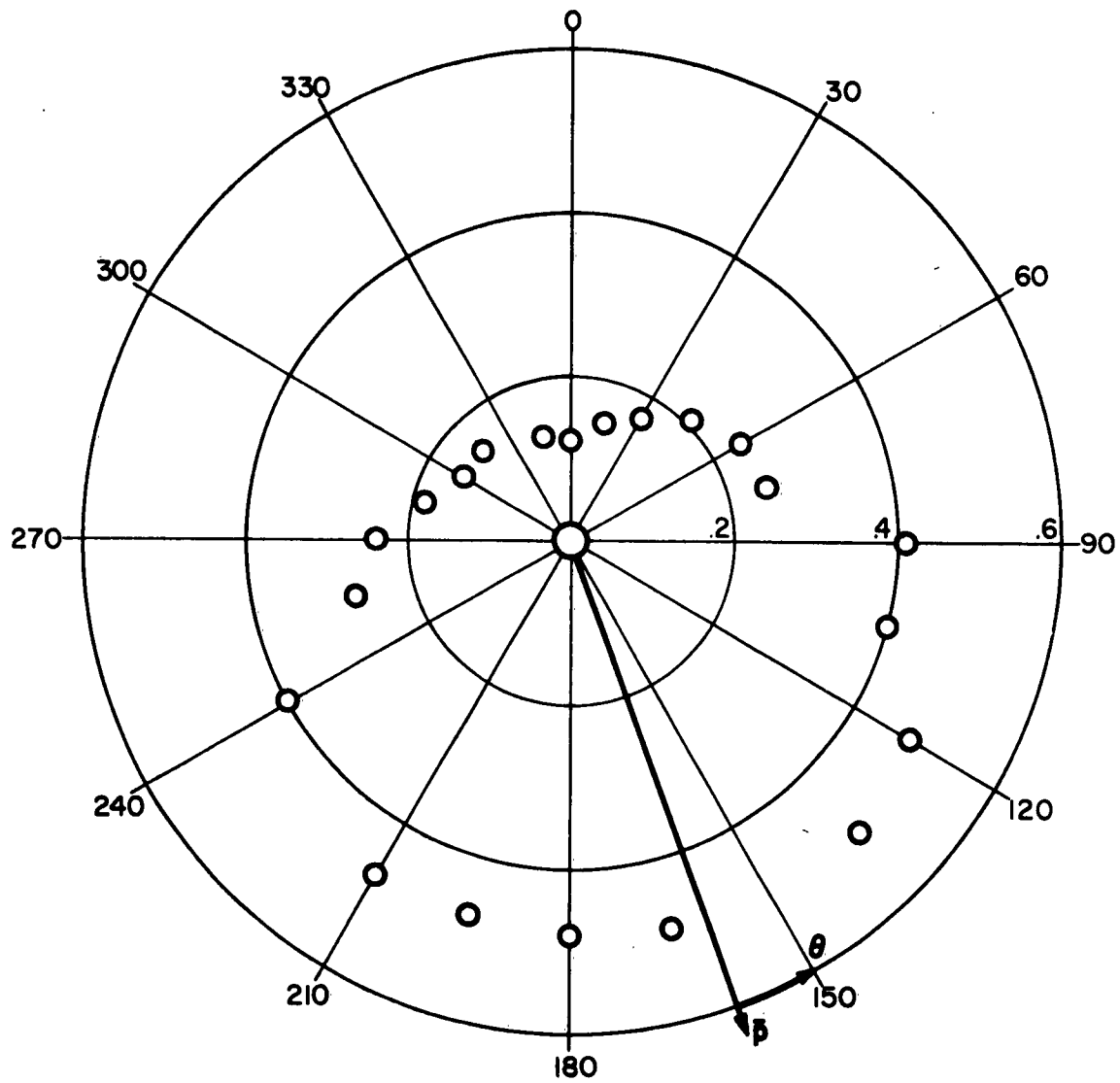


Fig. 4f. Circumferential Pressure Distribution -  $\bar{s} = 2.0$

and a Reynolds number parameter

$$\tilde{N}_r = N_r \left[ \frac{p_s}{\rho_{s_e} h_{s_e}} \right]^{\frac{1}{2}} = N_r \varphi_{s_e}^{\frac{1}{2}}$$

where

$$N_r = \rho_{s_e} \sqrt{h_{s_e}} R_o / \mu_{s_e} ; \varphi_{s_e} = p_s / \rho_{s_e} h_{s_e}$$

To facilitate instrumentation the thermocouples were placed in one plane only and the model rotated to obtain the distribution. Tests were made with the line of thermocouples in four planes. The Reynolds number range was covered in four tests to maintain as high a stagnation-to-wall enthalpy ratio as possible in any given test.

In order to prevent the shroud from reaching excessive temperatures, internal cooling was provided by means of an annular jet of high-pressure cold air, located at the minimum section of the shroud. Monitoring thermocouples were inserted on the exposed surface of the shroud and the temperature history recorded. During the tests it was found that the shroud temperature was within  $\pm 150^\circ\text{F}$  of the surface temperatures recorded on the conical portion of the model. On this basis no correction for radiation between the model and its surroundings is made. In the nose region, however, the model was subjected to radiation from the nozzle in which the shroud was installed. Estimates made in reference 21 indicate the increment in heat transfer is of the order of 10% of the total.

All tests were performed at a stagnation temperature in the range of  $1750^\circ\text{R}$  to  $1850^\circ\text{R}$ . The model stagnation pressure was varied from approximately 90 psia to 200 psia. The Reynolds number range covered was from about  $1.7 \times 10^6$  to  $3.7 \times 10^6$ .

The surface temperature measurements are believed to be accurate to within  $\pm 2\%$ . Errors in the stagnation temperature measurements are approximately 1.0%. These include the effect of recorder accuracy, reading error, and the possibility of the thermocouple junction being

slightly below the surface. An overall evaluation of the accuracy of the heat transfer data will be made in a later section.

### SECTION III

#### THEORETICAL ANALYSIS

##### A. Coordinate System

The coordinates with respect to the body axis are  $\varphi$  and  $\theta$ . The angle  $\varphi$  is measured along generators of the sphere from the axis of the body. The coordinate in the circumferential direction ( $\theta$ ), i. e., in planes perpendicular to the body axis, is measured from the windward generator of the body.

We also define a wind axis coordinate system ( $\psi, \beta$ ) where  $\psi$  is measured along generators of the sphere from the stagnation point, and  $\beta$  is measured, in planes perpendicular to the stream velocity, from the windward generator of the body. The transformation from body axes to wind axes is given by

$$\cos \psi = \cos \varphi \cos \alpha + \sin \varphi \sin \alpha \cos \theta$$

and

$$\cos \beta = \frac{1}{\sin \psi} [\cos \alpha \sin \varphi \cos \theta - \cos \varphi \sin \alpha]$$

##### B. Stagnation Point Location

The model was placed in the shroud at a geometric angle of attack of approximately  $1.5^\circ$  (Figure 1). The angle of attack to which this corresponds in terms of the flow field and the location of the stagnation point was determined from the measured pressure distribution. It has been found in the past that the pressure distribution, nondimensionalized with respect to the stagnation pressure, in the stagnation region of such a body in a shroud is best correlated by

$$\bar{p} = (1 - K') + K' \cos^2 \psi$$

where  $K'$  is an experimentally determined constant. In terms of the body axis coordinates this becomes

$$\bar{p} = (1 - K') + K'[\cos \varphi \cos \alpha + \sin \varphi \sin \alpha \cos \theta]^2$$

From the measured pressure distribution it was found that the pressure data was correlated to  $\varphi \approx .3$  with  $K' = 3.0$  and  $\alpha = 4^\circ$ . The pressure distribution in the stagnation region is therefore approximated by

$$\bar{p} = -2 + 3 [.998 \cos \varphi + .0698 \sin \varphi \cos \theta]^2$$

and the streamlines were assumed to be radial to the line defined by  $\varphi = 0.3$ .

### C. Streamline Location

As pointed out in the introduction, under the assumption of zero crossflow in the boundary layer, two-dimensional solutions can be applied along the streamlines external to the boundary layer. Two methods suggested for the determination of the location of the streamlines will be discussed here. The first by Vaglio-Laurin (reference 4) will be described briefly. The second, originally suggested by Ferri, was presented by Sanlorenzo (reference 13) and will be used in the present analysis.

In both cases the pressure distribution must be known, either from experiment or from approximate theoretical estimates. With the method of Vaglio-Laurin the streamline can then be obtained by a step-by-step process starting at a point where the velocity direction is known. A locus of such initial points on a blunt body could be chosen as a curve enclosing the stagnation point. Then, from the momentum equation in the direction normal to the streamline in the tangent plane of the body surface, the component of streamline curvature in the tangent plane can be determined. This quantity also determines the plane osculating the streamline at that point. The streamline is then approximated, for a small distance away from the initial point, by the line of intersection of the osculating plane and the body surface. The desired accuracy would of course determine the increment used. Thus, an adjacent point on the streamline

is found at which the process can be repeated.

The method of reference 13 incorporates several engineering approximations into the streamline calculation, and so makes it more amenable to numerical calculation. With a conical coordinate system we define

$$\begin{aligned}\bar{v}_r &= \bar{v}_0 + \bar{v}_1 \cos \theta \\ \bar{w} &= \bar{w}_1 \sin \theta\end{aligned}\tag{1}$$

where

$\bar{v}_r$  is the radial velocity component  
 $\bar{v}_n \neq 0$  is the velocity component normal to the body  
 $\bar{w}$  is the velocity component normal to free stream  
 $\theta$  is the peripheral angle measured from the windward meridian in a plane perpendicular to the body axis.

$\bar{v}_0, \bar{v}_1, \bar{w}_1$  are velocity perturbation coefficients

At any point on the body we can write

$$(\bar{v})^2 = 1 - (\bar{p})^{\frac{\gamma-1}{\gamma}}\tag{2}$$

where

$$\bar{v} = \frac{v}{v_m}, \quad v_m = \frac{2\gamma}{\gamma-1} \frac{p_s}{\rho_s}, \quad \bar{p} = \frac{p}{p_s}$$

and

$$\bar{v}^2 = \bar{v}_r^2 + \bar{w}^2$$

Substituting for  $\bar{v}$  in terms of its components we have an expression

relating the coefficients  $\bar{v}_0$ ,  $\bar{v}_1$  and  $\bar{w}_1$  to the pressure. Using the known pressure distribution and choosing three values of  $\theta$ , Eq. (2) may be solved simultaneously, to obtain, at each axial station of the cone, the coefficients  $\bar{v}_0$ ,  $\bar{v}_1$ , and  $\bar{w}_1$  that are consistent with the pressure distribution. Having thus established the velocity components at any point on the body it is possible to compute the direction of the streamline at that point. The streamline direction is given by

$$\epsilon = \tan^{-1} \frac{\bar{w}}{\bar{v}_r}$$

The computed value of  $\epsilon$  permits the determination of the location of an adjacent point at the next chosen station, where the calculation is repeated with the  $\theta$  and perturbation coefficients appropriate to the second station.

In the present case the above procedure was started at the line  $\varphi = 0.3$ , since the direction of the streamlines between the stagnation point and this line was taken to be radial ( $\beta = \text{const.}$ ). Five streamlines were calculated. On the line  $\varphi = 0.3$  the calculations were started at  $\theta$  equal to  $30^\circ$ ,  $60^\circ$ ,  $90^\circ$ ,  $120^\circ$ , and  $150^\circ$ .

The values obtained for the perturbation coefficient is shown in Figure 5. The streamline coordinates are shown in Tables 1 and 2.

#### D. Heat Transfer

The laminar heat transfer data will be compared to the theory of Lees modified for the more accurate stagnation point theory of Fay, Riddell, and Kemp. In terms of the Nusselt and Reynolds numbers used here we have

$$\frac{\text{Nu}}{N_r^{1/2}} = 0.398 \left( \frac{\rho_w \mu_w}{\rho_s \mu_s} \right)^{0.1} \frac{\bar{\rho} \bar{\mu} \bar{v} \bar{h}_2}{\varphi_s^{1/4} \left[ \int_0^s \bar{\rho} \bar{\mu} \bar{v} (\bar{h}_2)^2 d\tilde{s} \right]^{1/2}}$$

where  $h_2$  is the metric of a streamline coordinate system as defined in

# PERTURBATION COEFFICIENTS

$V_0, V_1, W_1$

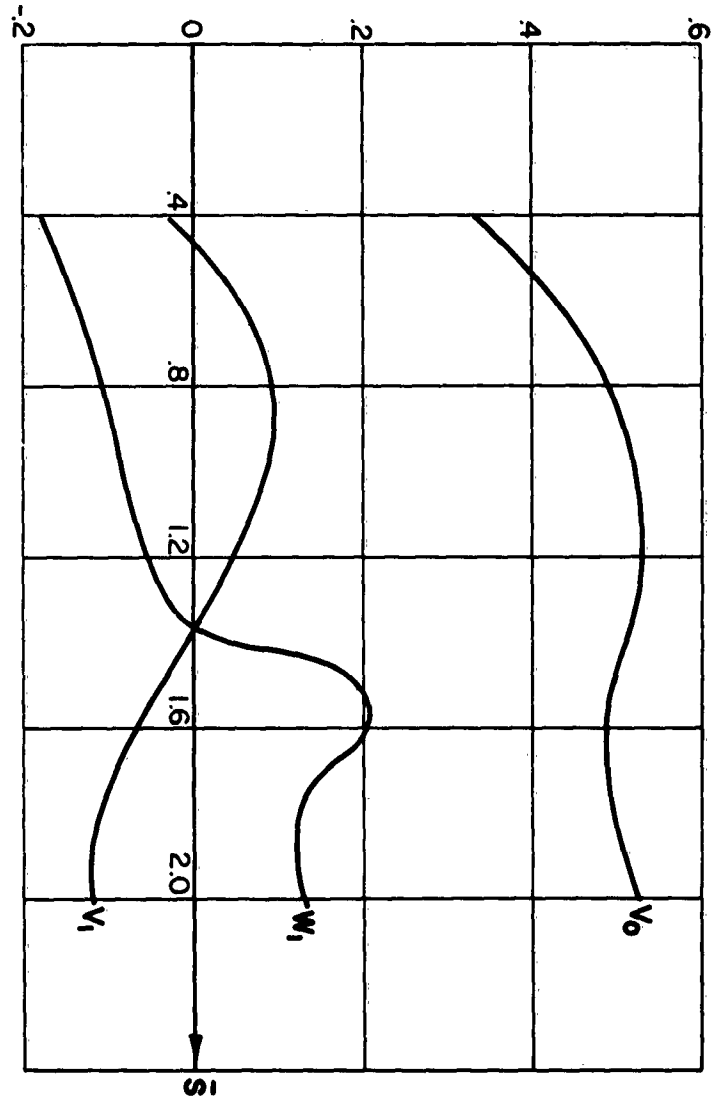


Fig. 5. Perturbation Coefficients

**TABLE 1**  
**LOCATION OF PRESSURE TAPS AND THERMOCOUPLES**

ROW	PRESSURE TAPS							THERMOCOUPLES			
	TAP NO.	S(in.)	1	2	3	4	5	6	7	NO.	DEGREES & S
0	0	0								0	0
1	0.20	1							1	1, 2	10°
2	0.42	2				2			2	3, 4	20°
3	0.63	3			3		3		3	5, 6	30°
4	0.89	4			4		4		4	7, 8	40°
5	1.14	5								9, 10	50°
6	1.36	6	6							11, 12	60°
7	1.59	7								13, 14	2.87
8	1.80	8	8	8	8	8	8	8	8	15, 16	3.12
9	2.03	9								17, 18	3.37
10	2.26	10	10							19, 20	3.62
11	2.46	11								21, 22	3.87
12	2.69	12	12	12	12	12	12	12	12	23, 24	4.12
13	2.92	13								25, 26	4.37
14	3.18	14	14							27, 28	4.62
15	3.43	15								29, 30	4.87
16	3.68	16	16	16	16	16	16	16	16	31, 32	5.12
17	3.92	17									
18	4.18	18	18								
19	4.43	19									
20	4.67	20	20	20	20	20	20	20	20		
21	4.92	21									
22	5.18	22	22								
23	5.42	23									

TABLE 2.0  
STREAMLINE COORDINATES

$\varphi_0 = .3$		$\varphi_0 = .3$		$\varphi_0 = .3$		$\varphi_0 = .3$		$\varphi_0 = .3$	
$\theta_0 = .523(30^\circ)$		$\theta_0 = 1.047(60^\circ)$		$\theta_0 = 1.571(90^\circ)$		$\theta_0 = 2.094(120^\circ)$		$\theta_0 = 2.618(150^\circ)$	
$\theta$	$\varphi(\bar{s})$	$\theta$	$\varphi(\bar{s})$	$\theta$	$\varphi(\bar{s})$	$\theta$	$\varphi(\bar{s})$	$\theta$	$\varphi(\bar{s})$
.560	.4	1.10	.40	1.638	.4	2.142	.4	2.648	.4
.562	.497	1.10	.494	1.64	.493	2.14	.495	2.63	.498
.517	.595	1.027	.588	1.559	.585	2.07	.589	2.58	.596
.491	.694	.979	.684	1.501	.680	2.016	.684	2.545	.694
.474	.793	.948	.782	1.458	.776	1.975	.781	2.518	.792
.462	.893	.924	.881	1.427	.874	1.944	.878	2.497	.891
.452	.993	.907	.980	1.403	.972	1.919	.977	2.480	.990
.445	1.092	.892	1.08	1.383	1.07	1.899	1.075	2.465	1.090
.440	1.192	.882	1.178	1.370	1.169	1.885	1.174	2.456	1.190
.436	1.292	.875	1.278	1.36	1.269	1.876	1.274	2.449	1.29
.434	1.392	.871	1.378	1.354	1.368	1.871	1.374	2.446	1.389
.437	1.492	.874	1.478	1.355	1.468	1.873	1.474	2.450	1.489
.451	1.59	.896	1.574	1.380	1.564	1.898	1.569	2.468	1.587
.467	1.688	.923	1.668	1.411	1.656	1.926	1.662	2.486	1.693
.480	1.786	.946	1.764	1.438	1.750	1.948	1.758	2.499	1.783
.491	1.885	.964	1.861	1.458	1.846	1.965	1.855	2.508	1.882
.501	1.984	.980	1.958	1.474	1.944	1.979	1.953	2.516	2.336

Note:  $\theta_0, \varphi_0$  denote the point at which the streamline calculation is started.

reference 4, and  $\tilde{s}$  is the distance along the streamline, non-dimensionalized with respect to the body nose radius.

The fully developed turbulent heat transfer data will be compared to the prediction of the flat-plate reference-enthalpy method. With a constant Prandtl number and with the recovery effect introduced to the factor K, the pertinent equations are

$$\frac{Nu}{\tilde{N}_r \tilde{s}} = \frac{0.04 \sigma^{\frac{1}{2}}}{\phi_{s_e}^{0.4}} \left( \frac{\bar{\rho}' \sqrt{v \tilde{s}}}{\bar{\mu}'} \right)^{\frac{1}{2}} \frac{\bar{\mu}'}{\tilde{s}} K$$

where  $\bar{\rho}' = \rho' / \rho_{s_e}$ ,  $\bar{\mu}' = \mu' / \mu_{s_e}$  and the primed quantities are evaluated at the state corresponding to the reference enthalpy defined by

$$h' = 0.5 h_w + 0.22 \sigma^{\frac{1}{2}} h_{s_e} + (0.50 - 0.22 \sigma^{\frac{1}{2}}) h_e$$

The factor K is given by

$$K = 1 - (1 - \sigma^{\frac{1}{2}}) \left[ \frac{1 - \bar{h}}{1 - \bar{h}_w} \right]$$

The metric ( $\bar{h}_2$ ) of the streamline coordinate was approximated by first calculating two auxiliary streamlines in addition to the one along which the heat transfer was to be evaluated. The auxiliary streamlines, originating at values of  $\theta$  which are  $5^\circ$  to either side of the primary one, made it possible to estimate geometrically the length element  $\bar{h}_2$ . For example, for the streamline originating at  $\theta = 30^\circ$ , two auxiliary streamlines with initial points at  $\theta = 25^\circ$  and  $35^\circ$  were also calculated. The metric could then be evaluated at any point on the primary streamline by approximating the distance between the primary and auxiliary streamlines by a straight line.

## SECTION IV

### COMPARISON BETWEEN THEORY AND EXPERIMENTS

The measured pressure distribution is shown in Figures 4a-f. It is indicated that the plane of symmetry of the flow is not in the vertical plane but at an angle of approximately  $20^\circ$  to the vertical. This was due to the slight misalignment that existed between the model support and shroud. Since this condition is fixed, with provision for positive control of the location of the models on the support, its effect can be easily accounted for.

The overall accuracy of the heat transfer measurements, based on the self consistency of the data, is thought to be about  $\pm 15$  percent. With the technique used to cover the Reynolds number range, which consisted in decreasing the stagnation pressure in the tunnel, the accuracy obtainable on the forward portion of the model is poor. This is so because the enthalpy at the wall can increase as fast as or faster than the Reynolds number is decreasing. Thus, only the conical portion of the body, where the heat transfer rates are lower, has been considered.

The measured heat transfer ( $Nu$  vs.  $\tilde{N}_r$ ) at twelve of the stations on the body are presented in Figures 6 through 9. Three data points in each of four axial planes ( $\theta = 20^\circ, 80^\circ, 100^\circ, 160^\circ$ ) are considered. The experimental results are compared to the values predicted by the flat-plate reference-enthalpy method. (Denoted by FPPE). For the purposes of comparison the prediction of the laminar theory is also shown for the three data points in the plane  $\theta = 80^\circ$  (Figure 7a-c). The theory was applied along five streamlines outside of the pitch plane, in addition to those in the pitch plane. The calculation was made at one-half inch increments along the streamlines and thus a fairly accurate estimate could be made for the values at data points which did not lie exactly on a calculated streamline. The results indicate that turbulent heating can be predicted fairly accurately in a three-dimensional boundary layer when the two-dimensional theory is applied along streamlines.

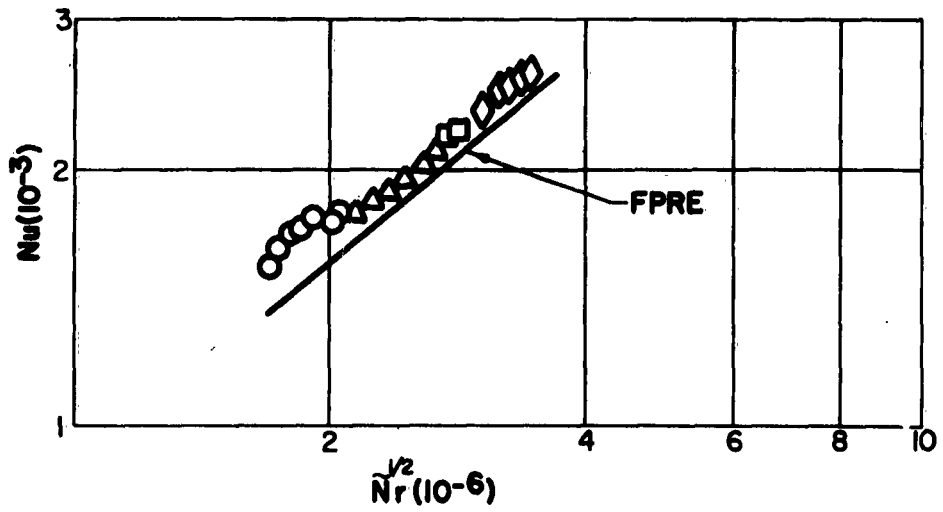


Fig. 6a. Nu vs.  $\tilde{N}_r$ ,  $\theta = 20^\circ$  - Thermocouple 21, ( $\bar{s} = 1.45$ )

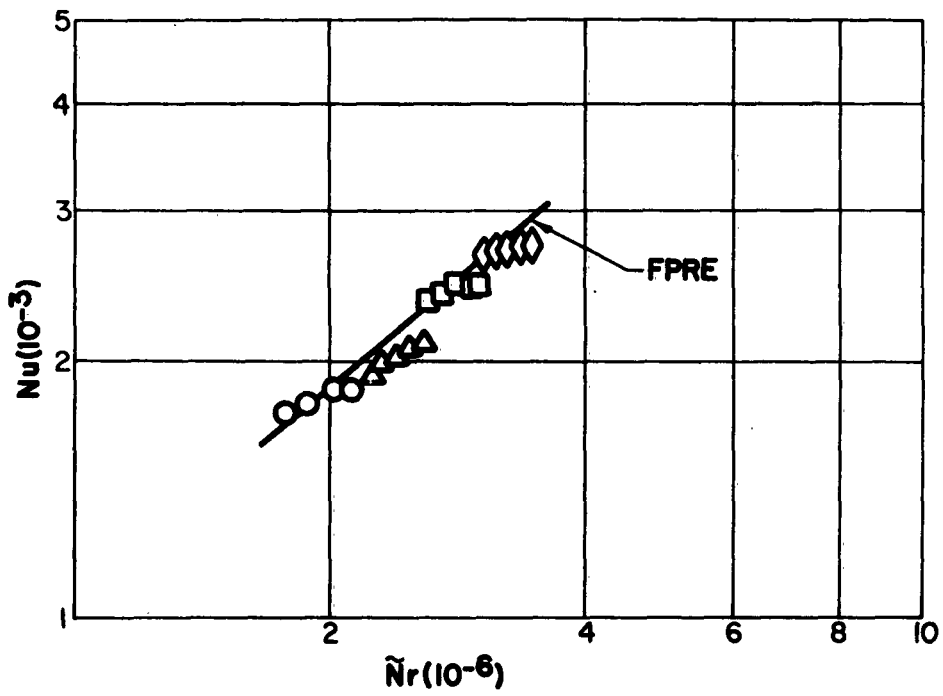


Fig. 6b. Nu vs.  $\tilde{N}_r$ ,  $\theta = 20^\circ$  - Thermocouple 25, ( $\bar{s} = 1.65$ )

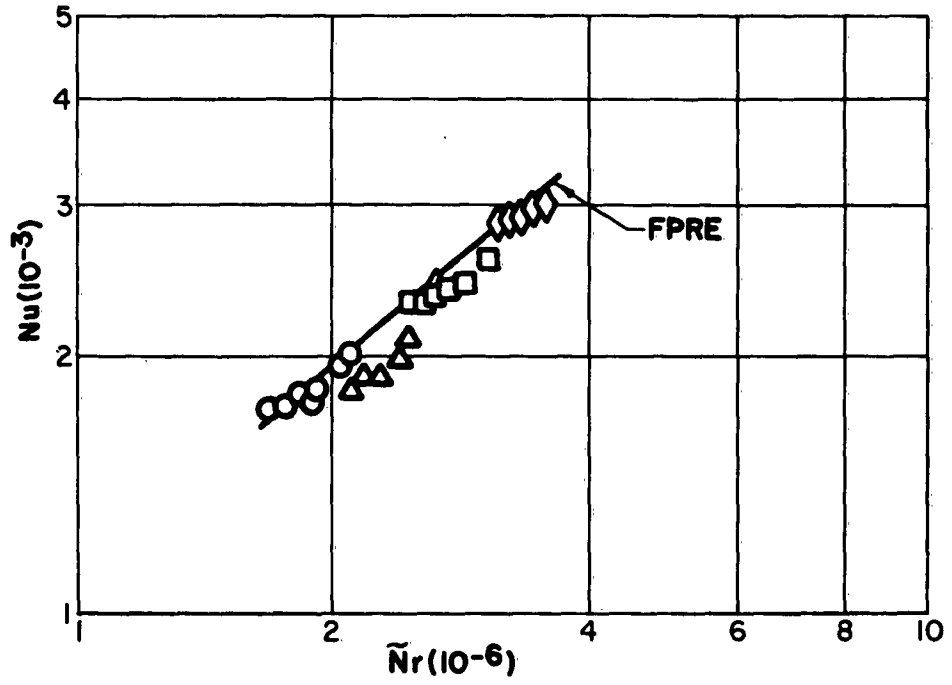


Fig. 6c. Nu vs.  $\tilde{N}_r$ ,  $\theta = 20^\circ$  - Thermocouple 27, ( $s = 1.75$ )

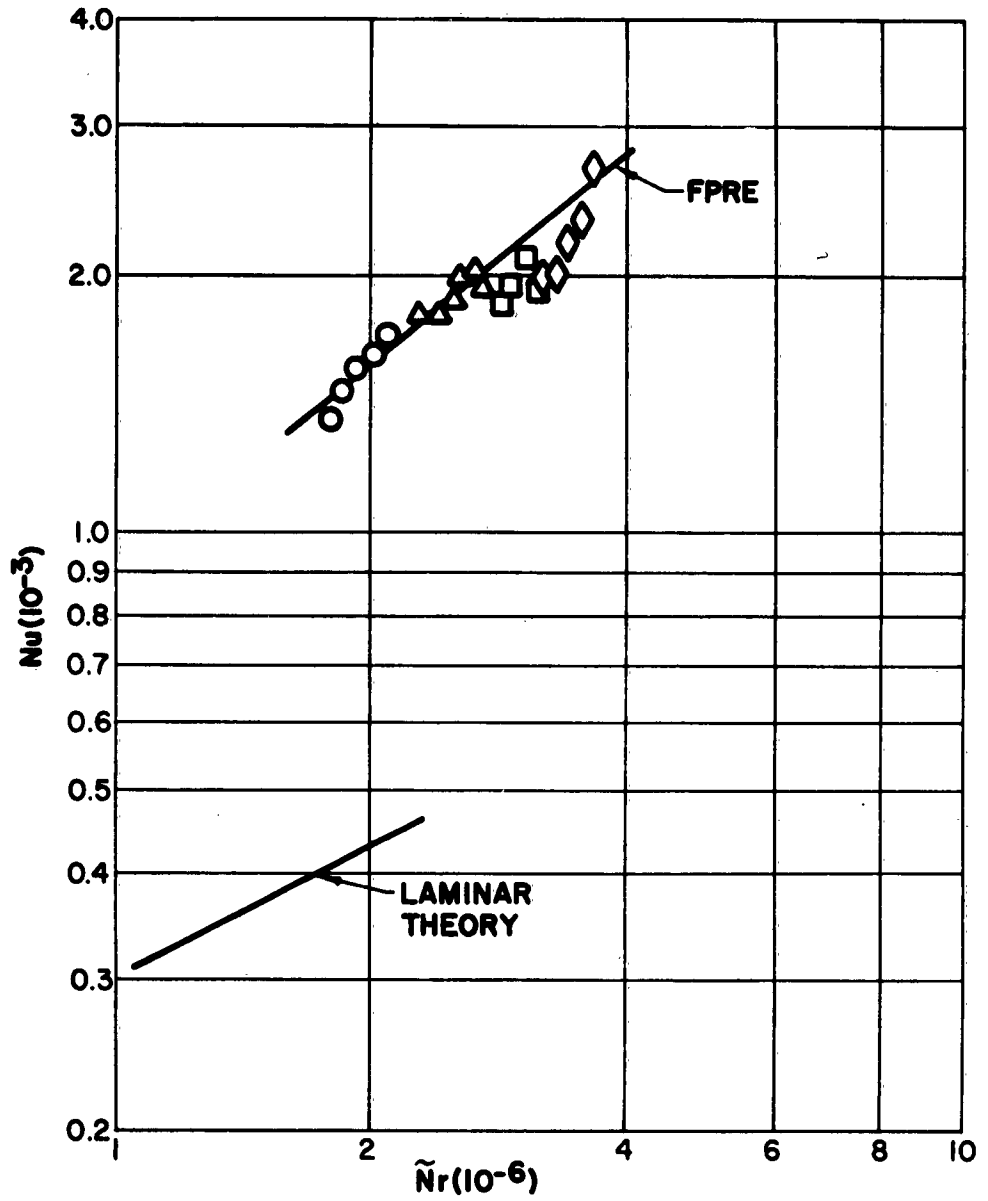


Fig. 7a.  $Nu$  vs.  $\tilde{N}_r$ ,  $\theta = 80^\circ$  - Thermocouple 17,  $(\bar{s} = 1.25)$

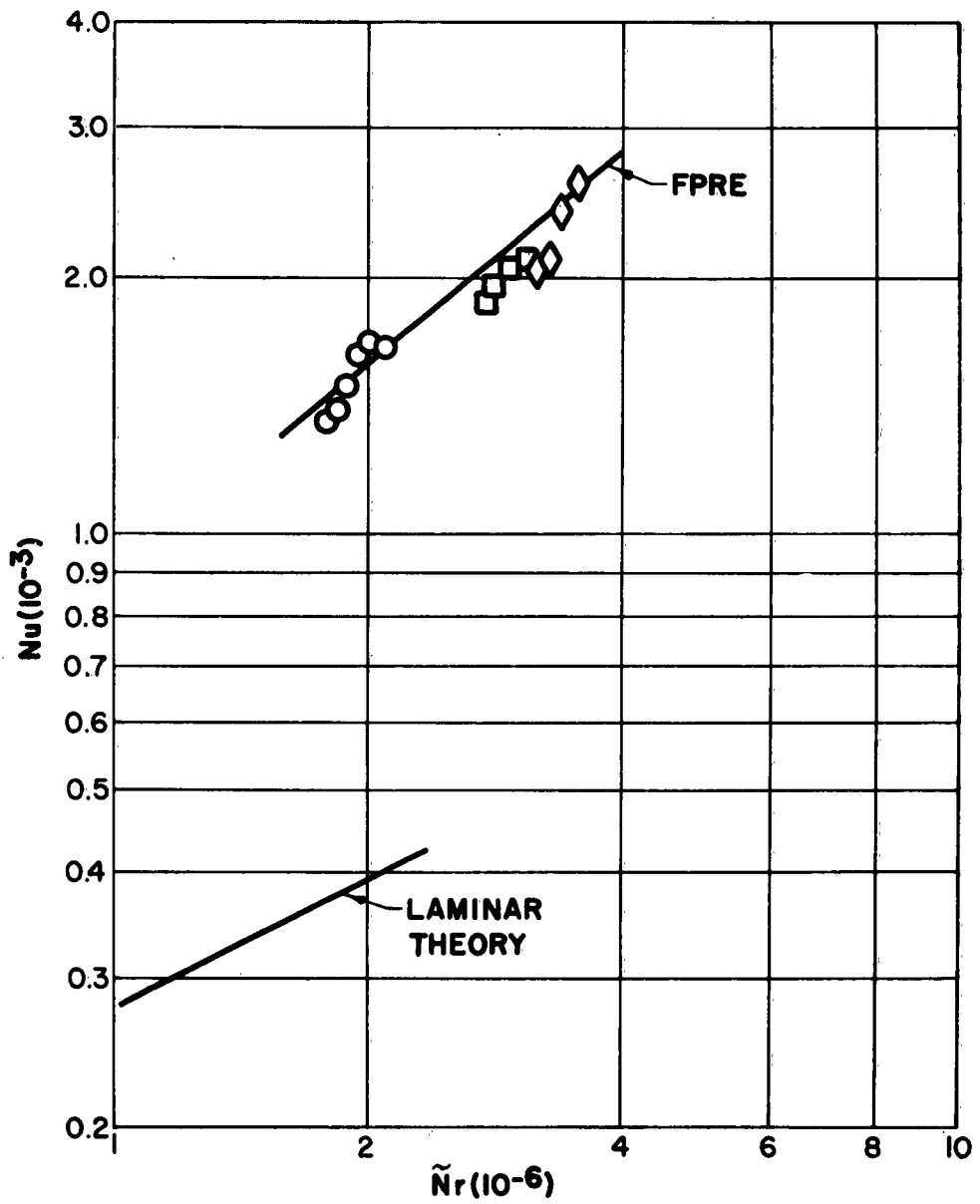


Fig. 7b.  $Nu$  vs.  $\tilde{N}_r$ ,  $\theta = 80^\circ$  - Thermocouple 25, ( $\bar{s} = 1.65$ )

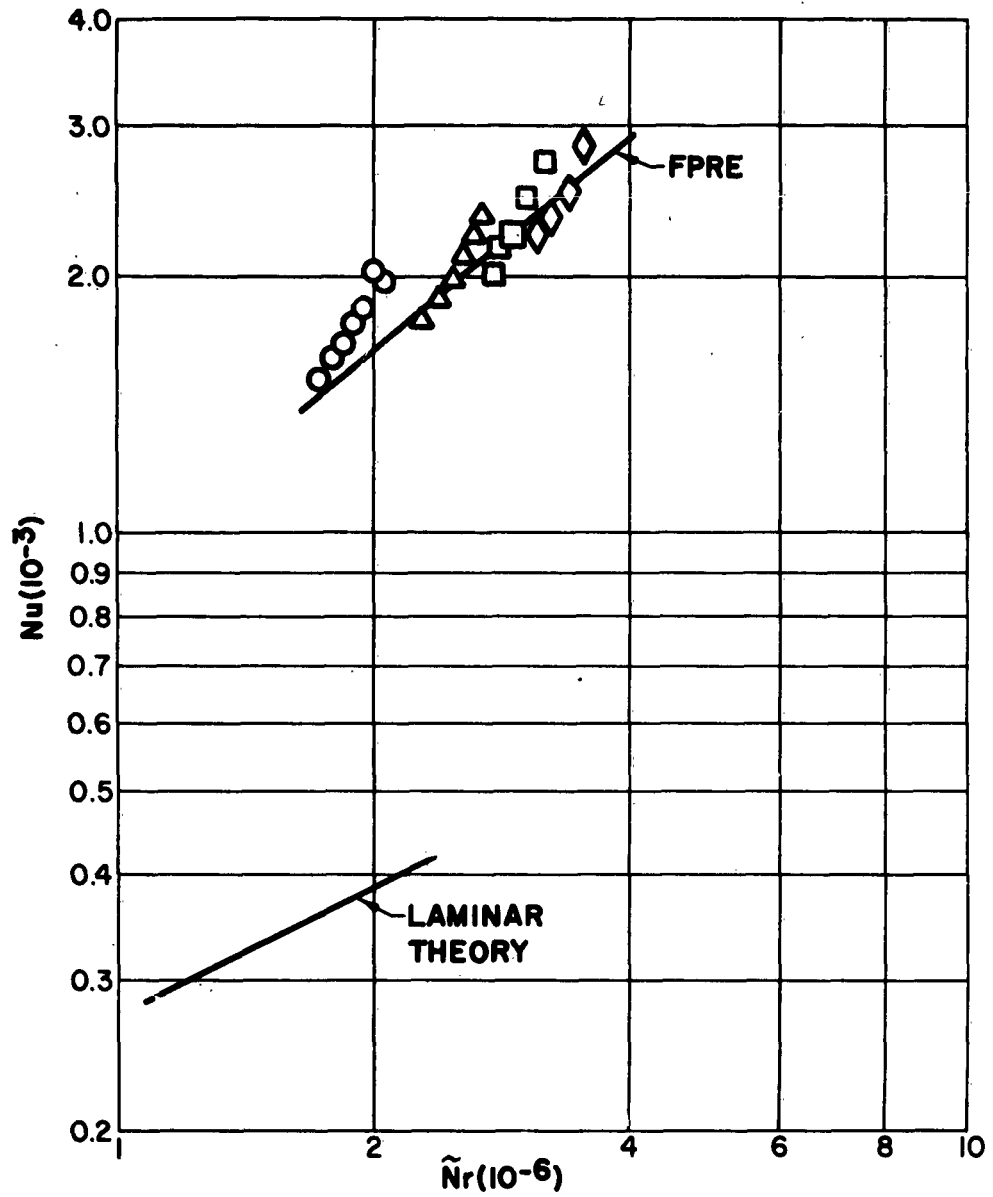


Fig. 7c. Nu vs.  $\tilde{N}_r$ ,  $\theta = 80^\circ$  - Thermocouple 27, ( $s = 1.75$ )

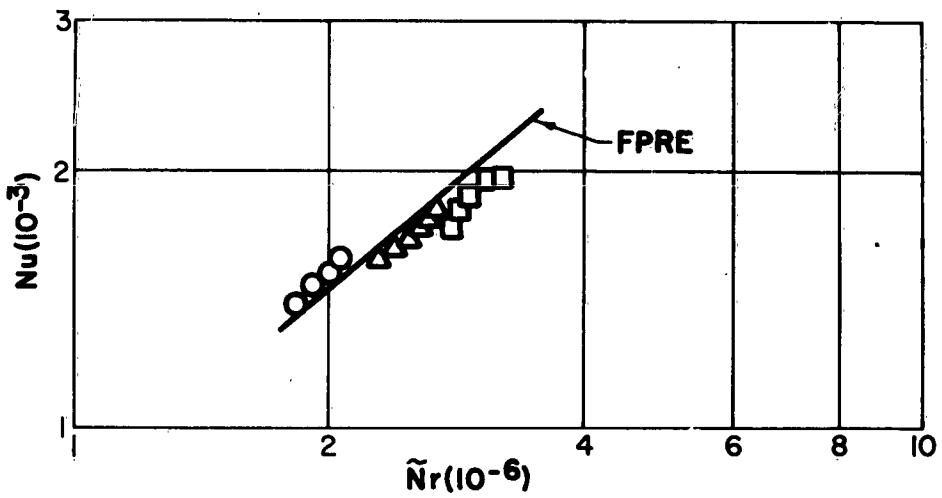


Fig. 8a.  $Nu$  vs.  $\tilde{N}_r$ ,  $\theta = 100^\circ$  - Thermocouple 22, ( $\bar{s} = 1.55$ )

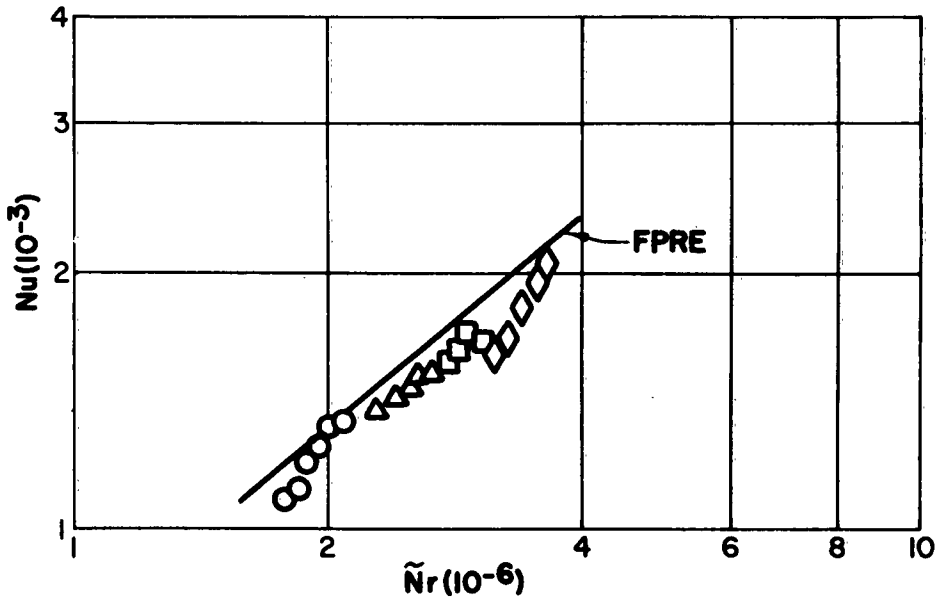


Fig. 8b.  $Nu$  vs.  $\tilde{N}_r$ ,  $\theta = 100^\circ$  - Thermocouple 30, ( $\bar{s} = 1.95$ )

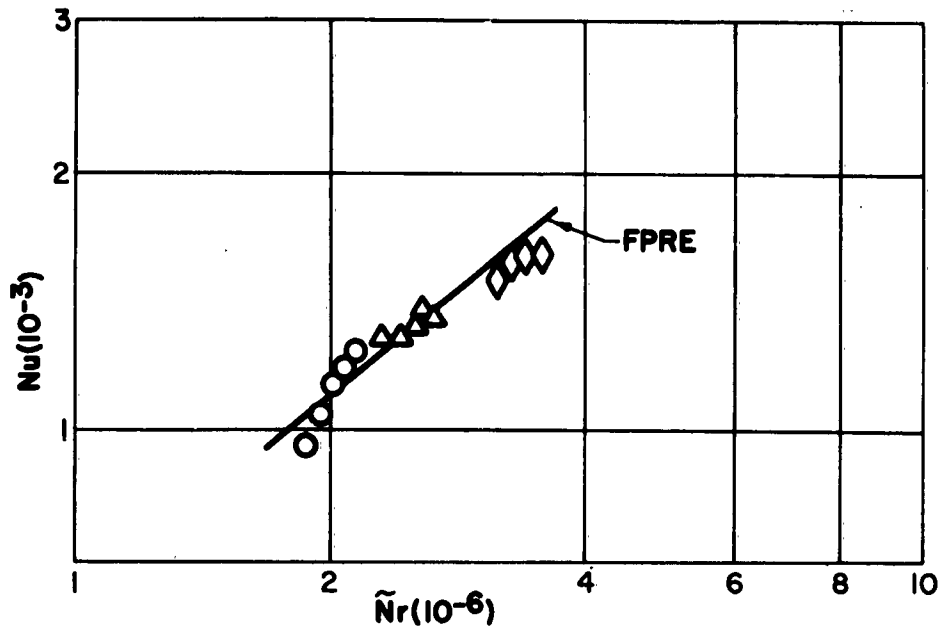


Fig. 8c.  $Nu$  vs.  $\tilde{N}_r$ ,  $\theta = 100^\circ$  - Thermocouple 32, ( $\bar{s} = 2.05$ )

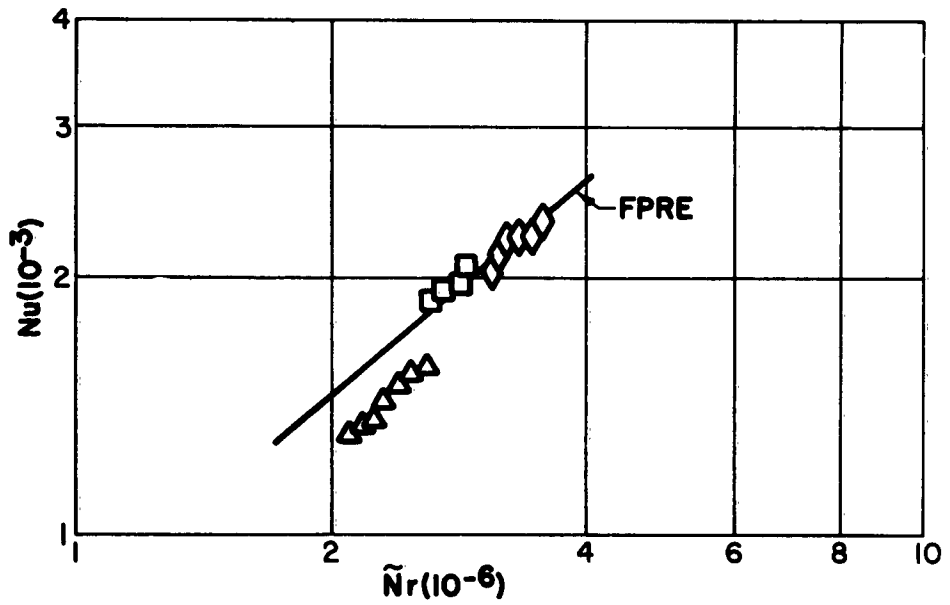


Fig. 9a.  $Nu$  vs.  $\tilde{N}_r$ ,  $\theta = 160^\circ$  - Thermocouple 20, ( $\bar{s} = 1.45$ )

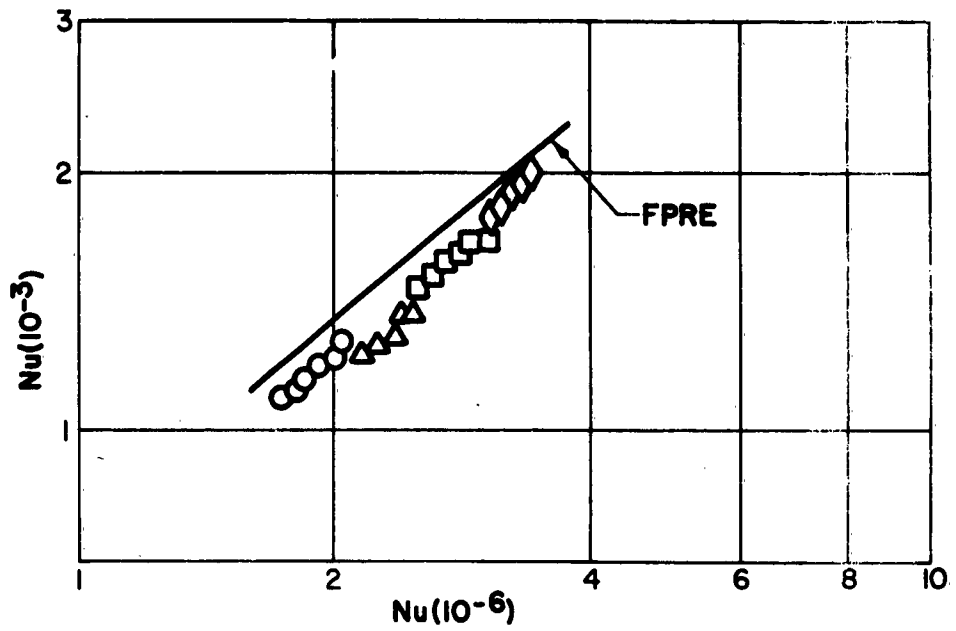


Fig. 9b.  $Nu$  vs.  $\tilde{N}_r$ ,  $\theta = 160^\circ$  - Thermocouple 22, ( $\bar{s} = 1.55$ )

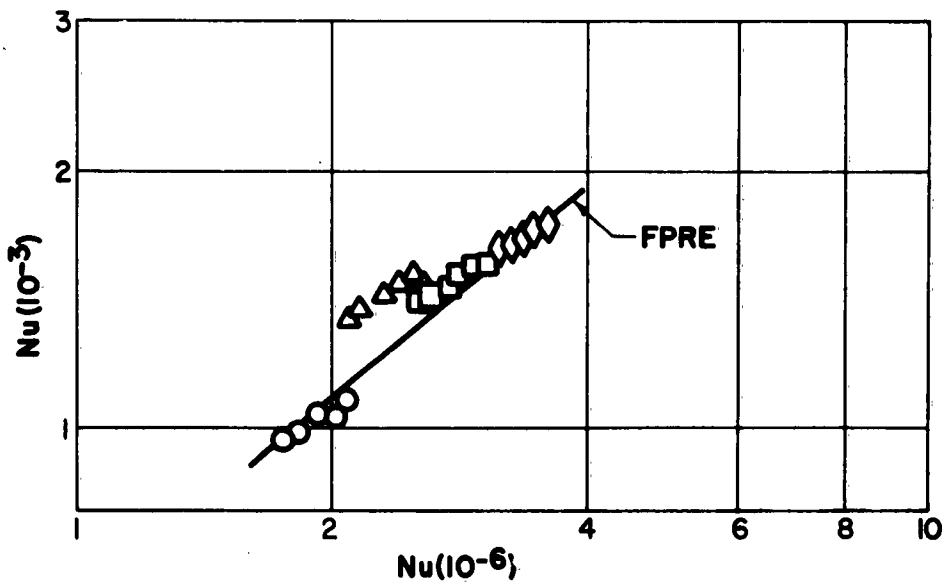


Fig. 9c.  $Nu$  vs.  $\tilde{N}_r$ ,  $\theta = 160^\circ$  - Thermocouple 26, ( $\bar{s} = 1.75$ )

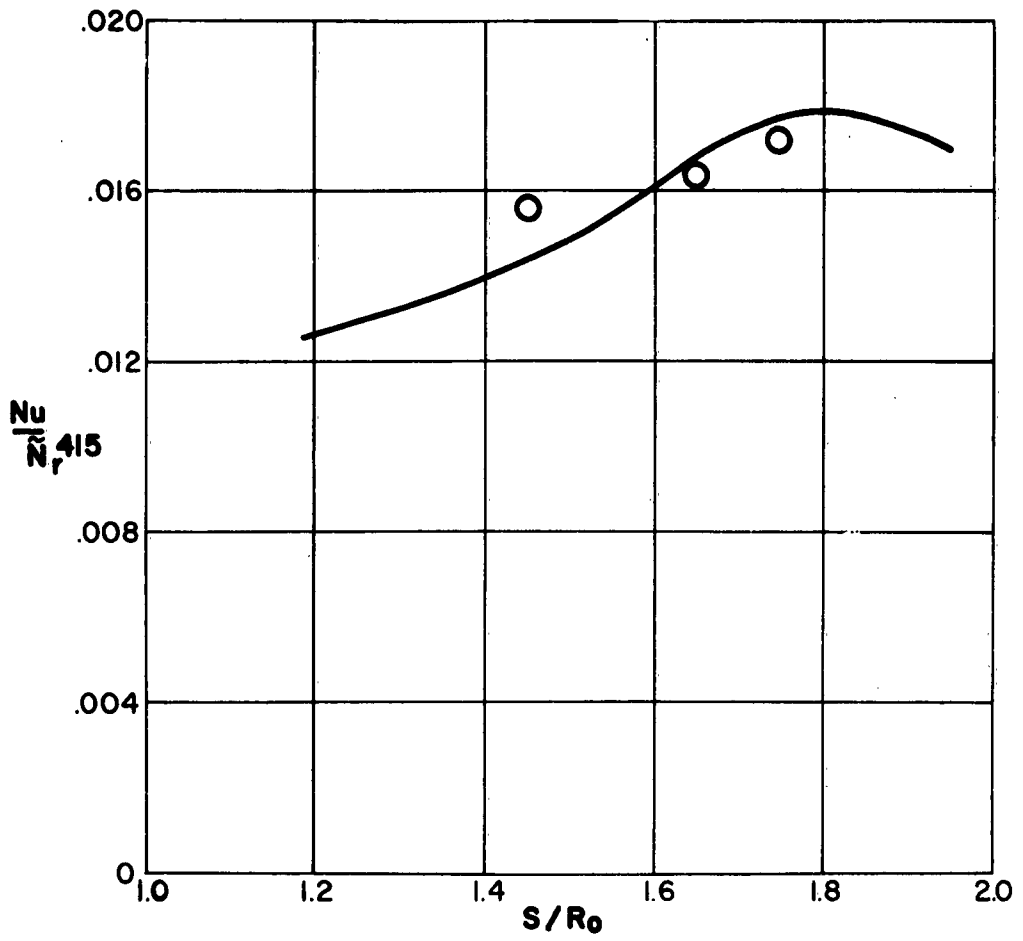


Fig. 10a.  $Nu/\tilde{N}_r^{4/5}$  vs.  $\bar{S}$  -  $\theta = 20^\circ$

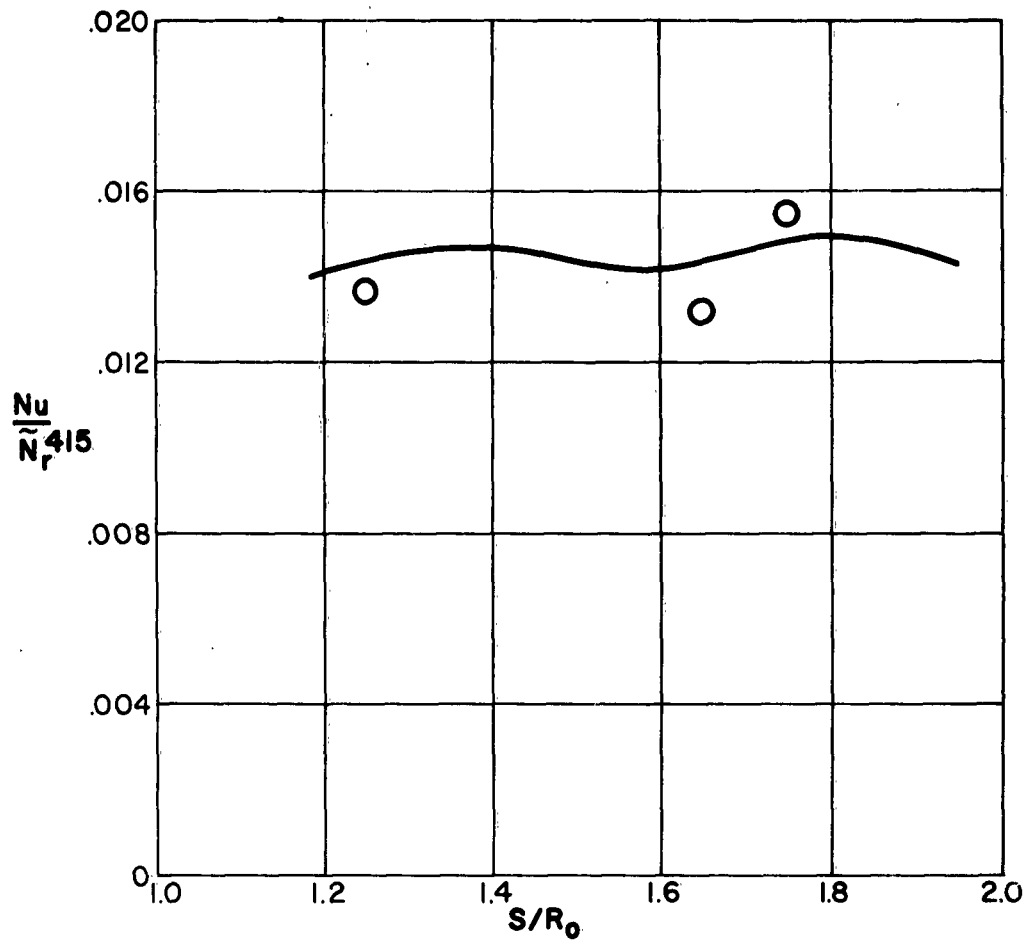


FIG. 10b.  $Nu/N_r^{4/5}$  vs.  $\bar{s}$  -  $\theta = 80^\circ$

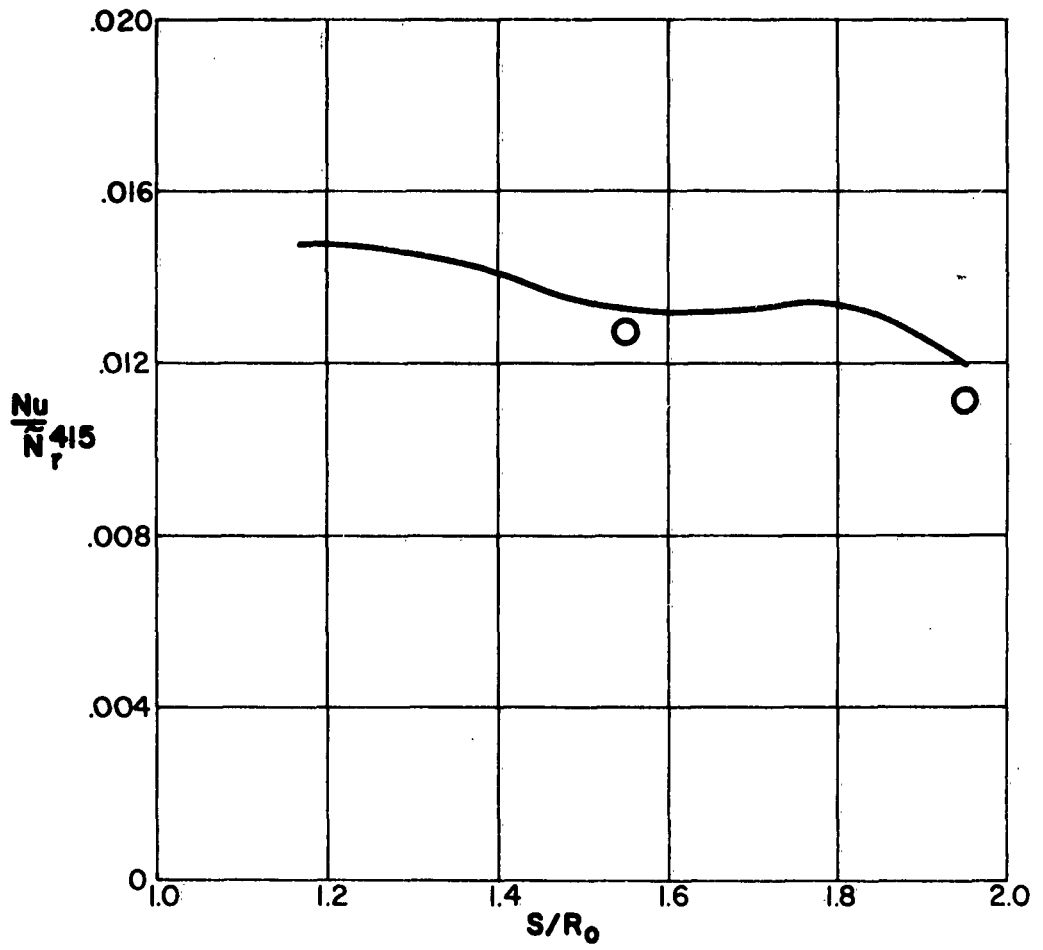


Fig. 10c.  $Nu/\tilde{N}_r^{4/5}$  vs.  $\bar{s}$  -  $\theta = 100^\circ$

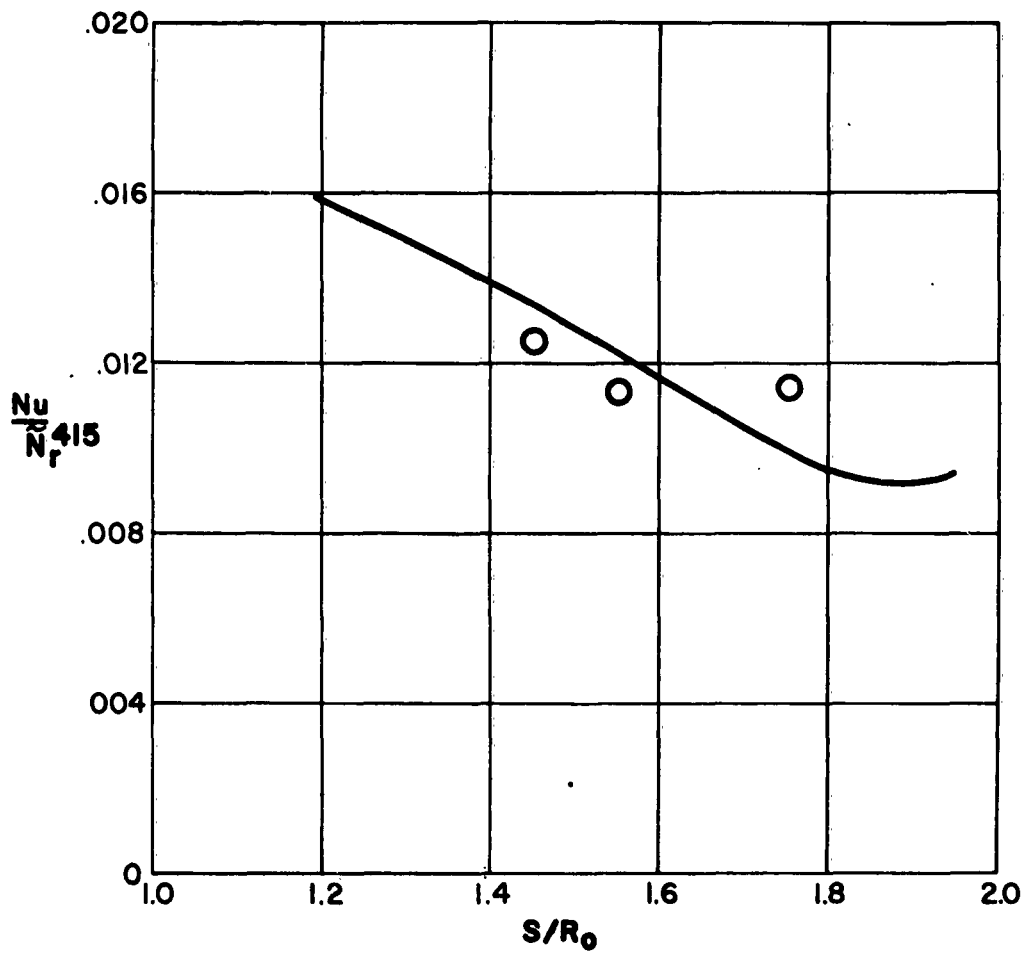


Fig. 10d.  $Nu/\tilde{N}_r^{0.415}$  vs.  $\bar{s}$  -  $\theta = 160^\circ$

The theoretical variation of  $Nu/N_r^{\frac{1}{2}}$  for the planes  $\theta = 20^\circ, 80^\circ, 100^\circ,$  and  $160^\circ$  is presented in Figures 10a-d. The values obtained experimentally at the various data points are also indicated.

## SECTION V

### CONCLUSIONS

This investigation has provided turbulent heat-transfer data for a range of Reynolds numbers from  $1.7 \times 10^6$  to  $3.7 \times 10^6$  and with enthalpy ratios on the order of two. The data has been obtained on a spherically capped cone at angle of attack with the shrouded model technique. A comparison of experimental results shows that the flat-plate reference-enthalpy theory applied along inviscid streamlines, provides a relatively accurate estimate of turbulent heating rates in a three-dimensional boundary layer.

## SECTION VI

### REFERENCES

1. Lees, L.: Laminar Heat Transfer Over Blunt-Nosed Bodies at Hypersonic Flight Speeds. Jet Propulsion, 26, pp. 259-269, April 1956.
2. Probstein, R. F.: Method of Calculating the Equilibrium Laminar Heat Transfer Rate at Hypersonic Flight Speeds. Jet propulsion, 26, pp. 497-499, June 1956.
3. Fay, J. A. and Riddell, F. R.: Theory of Stagnation Point Heat Transfer in Dissociated Air. J. Aero. Sci., 25, pp. 73-85, February 1958.
4. Vaglio-Laurin, R.: Laminar Heat Transfer on Blunt-Nosed Bodies in Three-Dimensional Hypersonic Flow. WADC TN 58-147, AD 155 588, May 1958.

5. Hayes, W. D.: The Three-Dimensional Boundary Layer. NAVORD Report No. 1313, U. S. Naval Ord. Test Station, Inyokern, May 1951.
6. Moore, F. K.: Three-Dimensional Compressible Laminar Boundary Layer Flow. NACA TN 2279, March 1951.
7. Howarth, L.: The Boundary Layer in Three-Dimensional Flow. Part I. Derivation of the Equations for Flow Along a General Curved Surface. Philosophical Magazine, Series 7, Vol. 42, pp. 239-243, 1951.
8. Moore, F. K.: Three-Dimensional Boundary Layer Theory. Vol. IV, Advances in Applied Mechanics, pp. 159-228, Academic Press, 1956.
9. Reshotko, E. and Beckwith, I. E.: Compressible Laminar Boundary Layer Over a Yawed Infinite Cylinder with Heat Transfer and Arbitrary Prandtl Number. NACA TN 3986, June 1957.
10. Reshotko, E.: Laminar Boundary Layer with Heat Transfer on a Cone at Angle of Attack in a Supersonic Stream. NACA TN 4152, December 1957.
11. Reshotko, E.: Heat Transfer to a General Three-Dimensional Stagnation Point. Jet Propulsion, 28, 1, pp. 58-60, January 1960.
12. Vaglio-Laurin, R.: Three-Dimensional Laminar Boundary Layer with Small Cross Flow About Blunt Bodies in Hypersonic Flight. GASL TR 59, April 1958.
13. Sanlorenzo, E.: Method for Prediction of Streamlines and Heat Transfer to Bodies in Hypersonic Flow. GASL Tech. Report No. 177.
14. Libby, P. A. and Cresci, R. J.: Evaluation of Several Hypersonic Turbulent Heat Transfer Analyses by Comparison with Experimental Data. WADC TN 57-72, AD 118 093, July 1957.
15. Englert, G. W.: Estimation of Compressible Boundary Layer Growth Over Insulated Surfaces with Pressure Gradient. NACA TN 4022, June 1957.
16. Mager, A.: Transformation of the Compressible Turbulent Boundary Layer. J. Aero. Sci., 25, 5, pp. 305-311, May 1958
17. Mager, A.: Generalization of Boundary Layer Momentum Integral Equations to Three-Dimensional Flows Including Those of Rotating Systems. NACA Report 1067, 1952.
18. Braun, W. H.: Turbulent Boundary Layer on a Yawed Cone in a Supersonic Stream. NACA TN 4208, January 1958.

19. Vaglio-Laurin, R.: Turbulent Heat Transfer on Blunt-Nosed Bodies in Two-Dimensional and General Three-Dimensional Hypersonic Flow. WADC TN-58-301, AD 206 050, September 1958.
20. Ferri, A. and Libby, P. A.: A New Technique for Investigating Heat Transfer and Surface Phenomena Under Hypersonic Flow Conditions. J. Aero. Sci., 24, 6, pp. 464-465, June 1957.
21. Cresci, R. J., MacKenzie, D. A., and Libby, P. A.: An Investigation of Laminar, Transitional and Turbulent Heat Transfer on Blunt-Nosed Bodies in Hypersonic Flow. J. Aero. Sci., 27, 6, June 1960.
22. Beckwith, I. E. and Gallagher, J. J.: Heat Transfer and Recovery Temperature on a Sphere with Laminar, Transitional and Turbulent Boundary Layers at Mach Numbers of 2.00 and 4.15. NACA TN 4125, December 1957.
23. Ferri, A. and Libby, P. A.: The Hypersonic Facility of the Polytechnic Institute of Brooklyn and Its Application to Problems of Hypersonic Flight. WADC TR 57-369, AD 130 809, August 1957.
24. Bloom, M. H.: A High Temperature-Pressure Air Heater (Suitable for Intermittent Hypersonic Wind Tunnel Operation). WADC TN 55-694, AD 110 725, November 1956.

<p>Aeronautical Research Laboratories, Wright-Patterson AFB, O. AN INVESTIGATION OF A THREE-DIMENSIONAL TURBULENT BOUNDARY LAYER IN HYPersonic FLOW by Gennaro Aiello, PIB, Ffeoport, N. Y. February 1963. 39 p. incl. illus. (Project 7064-Task 7064-01) (Contract AF 33(616)-7661) (ARL 63-26)</p> <p>Unclassified Report</p> <p>Turbulent heating rates have been measured by means of the shrouded model technique on a blunted cone at angle of attack. The Reynolds number, based on conditions at the stagnation point, was varied from <math>1.7 \times 10^6</math> to approximately <math>3.7 \times 10^6</math>. The enthalpy ratio (stagnation to wall) varied from 2.1 to approximately 1.5.</p> <p>( over )</p>	<p>UNCLASSIFIED</p> <p>I. Hypersonic Aerodynamics</p> <p>2. Heat Transfer</p> <p>3. Turbulent Boundary Layer</p> <p>I. Gennaro F. Aiello</p> <p>II. Aeronautical Research Laboratories</p> <p>Contract AF 33(616)-7661</p> <p>UNCLASSIFIED</p>	<p>Aeronautical Research Laboratories, Wright-Patterson AFB, O. AN INVESTIGATION OF A THREE-DIMENSIONAL TURBULENT BOUNDARY LAYER IN HYPersonic FLOW by Gennaro Aiello, PIB, Ffeoport, N. Y. February 1963. 39 p. incl. illus. (Project 7064-Task 7064-01) (Contract AF 33(616)-7661) (ARL 63-26)</p> <p>Unclassified Report</p> <p>Turbulent heating rates have been measured by means of the shrouded model technique on a blunted cone at angle of attack. The Reynolds number, based on conditions at the stagnation point, was varied from <math>1.7 \times 10^6</math> to approximately <math>3.7 \times 10^6</math>. The enthalpy ratio (stagnation to wall) varied from 2.1 to approximately 1.5.</p> <p>( over )</p>	<p>UNCLASSIFIED</p> <p>I. Hypersonic Aerodynamics</p> <p>2. Heat Transfer</p> <p>3. Turbulent Boundary Layer</p> <p>I. Gennaro F. Aiello</p> <p>II. Aeronautical Research Laboratories</p> <p>Contract AF 33(616)-7661</p> <p>UNCLASSIFIED</p>	<p>UNCLASSIFIED</p> <p>The experimental data are compared to the flat-plate reference-enthalpy theory applied along the inviscid streamlines. It is shown that this relatively simple method is in reasonable agreement with the data.</p>
<p>UNCLASSIFIED</p> <p>1. Hypersonic Aerodynamics</p> <p>2. Heat Transfer</p> <p>3. Turbulent Boundary Layer</p> <p>I. Gennaro F. Aiello</p> <p>II. Aeronautical Research Laboratories</p> <p>Contract AF 33(616)-7661</p> <p>UNCLASSIFIED</p>	<p>Aeronautical Research Laboratories, Wright-Patterson AFB, O. AN INVESTIGATION OF A THREE-DIMENSIONAL TURBULENT BOUNDARY LAYER IN HYPersonic FLOW by Gennaro Aiello, PIB, Ffeoport, N. Y. February 1963. 39 p. incl. illus. (Project 7064-Task 7064-01) (Contract AF 33(616)-7661) (ARL 63-26)</p> <p>Unclassified Report</p> <p>Turbulent heating rates have been measured by means of the shrouded model technique on a blunted cone at angle of attack. The Reynolds number, based on conditions at the stagnation point, was varied from <math>1.7 \times 10^6</math> to approximately <math>3.7 \times 10^6</math>. The enthalpy ratio (stagnation to wall) varied from 2.1 to approximately 1.5.</p> <p>( over )</p>	<p>UNCLASSIFIED</p> <p>The experimental data are compared to the flat-plate reference-enthalpy theory applied along the inviscid streamlines. It is shown that this relatively simple method is in reasonable agreement with the data.</p>	<p>UNCLASSIFIED</p>	